

1 **Genomic data reveal a north-south split and introgression history of blood fluke**
2 **(*Schistosoma haematobium*) populations from across Africa**

3 Roy N Platt II¹, Egie E. Enabulele¹, Ehizogie Adeyemi², Marian O Agbugui³, Oluwaremilekun G
4 Ajakaye⁴, Ebube C Amaechi⁵, Chika E Ejikeugwu⁶, Christopher Igbeneghu⁷, Victor S Njom⁸,
5 Precious Dlamini⁹, Grace A. Arya¹, Robbie Diaz¹, Muriel Rabone¹⁰, Fiona Allan¹⁰, Bonnie
6 Webster¹⁰, Aidan Emery¹⁰, David Rollinson^{10, 11}, Timothy J.C. Anderson¹

7 ¹ Texas Biomedical Research Institute, San Antonio TX, United States

8 ² Department of Pathology, University of Benin Teaching Hospital, Edo State, Nigeria

9 ³ Department of Biological Sciences, Edo State University, Uzairue, Nigeria

10 ⁴ Department of Animal and Environmental Biology, Adekunle Ajasin University, Nigeria

11 ⁵ Department of Zoology, University of Ilorin, Kwara State, Nigeria

12 ⁶ Enugu State University of Science and Technology, Nigeria

13 ⁷ Department of Medical Laboratory Science, Ladoke Akintola University of Technology, Nigeria

14 ⁸ Department of Applied Biology and Biotechnology, Enugu State University of Science and
15 Technology, Nigeria

16 ⁹ Central Public Health Offices, Manzini, Swaziland

17 ¹⁰ Science Department, Natural History Museum, London, United Kingdom

18 ¹¹ Global Schistosomiasis Alliance, London, United Kingdom

19

20 **Keywords:** schistosomes, parasite, *Schistosoma haematobium*, *Schistosoma bovis*,
21 hybridization, introgression, desert, admixture

22 **Abstract:** The human parasitic fluke, *Schistosoma haematobium* hybridizes with the livestock
23 parasite *S. bovis* in the laboratory, but the frequency of hybridization in nature is unclear. We
24 analyzed 34.6 million single nucleotide variants in 162 samples from 18 African countries,

25 revealing a sharp genetic discontinuity between northern and southern *S. haematobium*. We
26 found no evidence for recent hybridization. Instead the data reveal admixture events that occurred
27 257-879 generations ago in northern *S. haematobium* populations. Fifteen introgressed *S. bovis*
28 genes are approaching fixation in northern *S. haematobium* with four genes potentially driving
29 adaptation. We identified 19 regions that were resistant to introgression; these were enriched on
30 the sex chromosomes. These results (i) suggest strong barriers to gene flow between these
31 species, (ii) indicate that hybridization may be less common than currently envisaged, but (iii)
32 reveal profound genomic consequences of rare interspecific hybridization between schistosomes
33 of medical and veterinary importance.

34 *Funding* - This work was funded by NIH NIAID (R01 AI166049).

35 **Introduction**

36

37 Hybridization and the transfer of alleles via introgression is an important source of genetic
38 variation between species¹. This process allows for allelic variants, which have already been
39 preselected in a donor species, to be introduced into the genome of a recipient species in a single
40 generation. By comparison, it may take multiple generations for random mutation and selection
41 to deliver comparable levels of genetic variation in the absence of introgression². As a result,
42 introgressive hybridization, can contribute to the evolution of new genetic traits in hybridizing
43 species³. Hybridization between human and animal pathogens can lead to the emergence of
44 parasites with novel traits such as increased pathogenicity⁴, expanded host range⁵, altered
45 transmission dynamics⁶ and drug resistance⁷. Understanding the frequency and impact of such
46 hybridization events is critical for devising effective disease intervention strategies.

47

48 Members of the blood fluke genus *Schistosoma* parasitize a range of mammal species and cause
49 substantial morbidity and economic loss⁸. Parasites in this genus have a complex life cycle: first-
50 stage larvae (miracidia) infect an aquatic snail intermediate host where they develop into
51 sporocysts. Clonally generated, motile second-stage larvae (cercariae) emerge from the
52 intermediate host, and actively locate and penetrate the skin of the definitive mammalian host. In
53 the mammal host, mature parasites form male-female pairs in the blood stream and reproduce
54 sexually. Eggs are excreted through the feces or urine, depending on the parasite species, which
55 restarts the life cycle.

56

57 One pair of species, *S. haematobium*, a human parasite, and *S. bovis*, an ungulate parasite
58 common in domestic livestock, are genetically divergent (3-5% and 18% divergent in the nuclear
59 and mitochondrial genomes respectively), but can hybridize and produce viable offspring when
60 given the opportunity⁹. Given the close proximity between humans and their livestock and the
61 regular use of the same water bodies, the potential for hybridization between these species is a
62 particular concern and a significant effort has been mounted to identify, monitor and map *S.*
63 *haematobium* and *S. bovis* hybrids¹⁰. Multiple studies have reported mitochondrial and/or
64 ribosomal DNA from *S. bovis* in *S. haematobium* populations. For examples see^{9,11-13}. The high
65 frequency of individuals with discordant mitochondrial and nuclear markers has been used to
66 argue that hybridization is common and that the zoonotic threat of *S. bovis* should be considered
67 in human schistosomiasis control programs¹⁴.

68

69 However, several, more recent multi-marker and genomic studies using single nucleotide variants
70 (SNVs), microsatellite markers and whole genome sequence assemblies have suggested that
71 hybridization between *S. haematobium* and *S. bovis* may not occur as frequently as previously
72 postulated. Exome¹⁵, whole genome¹⁶, and microsatellite data¹⁷, and others¹⁸⁻²¹ failed to identify
73 evidence of contemporary hybridization in field-collected parasites. Instead, these studies indicate
74 that *S. bovis* and *S. haematobium* are genetically distinct and do not hybridize frequently but
75 evidence for historical hybridization is clearly evident within genomes of *S. haematobium*. As a
76 result, some *S. bovis* genes have introgressed into the *S. haematobium* population and reached
77 high frequency; evidence of a potential, adaptive introgression event^{15,16,18,20}.

78
79 In this study, we build upon previous work and try to address knowledge gaps by analyzing a
80 comprehensive dataset of 34.6 million genome-wide SNVs from *S. bovis* (n=21) and *S.*
81 *haematobium* (n=141) samples collected from 18 countries across the African continent. Many of
82 these samples presented discordant mitochondrial and ribosomal DNA profiles and were
83 categorized as *S. haematobium-bovis* hybrids. This expanded dataset, and recent availability of
84 a high-quality *S. haematobium* genome assembly²², allows for a more detailed examination of the
85 genetic relationships between these two species and the potential consequences of hybridization
86 on their evolution and epidemiology. Our results: (i) reveal a strong discontinuity between northern
87 and southern *S. haematobium* populations; (ii) define similar genomic introgression profiles in *S.*
88 *haematobium* sampled from locations 3,002 Km apart; (iii) fine-map introgressed genome regions
89 and identify putative genes driving adaptive introgression; (iv) identify two distinct lineages of *S.*
90 *bovis*-like mitochondrial DNA in northern *S. haematobium*, consistent with historical introgression
91 and (v) identify “introgression deserts” on the ZW chromosomes consistent with the sex
92 chromosomes maintaining species integrity. These results enhance our understanding of
93 *Schistosoma* spp. epidemiology, with important implications for control efforts.

94
95 **Results**

96
97 DNA Sequencing and Genotyping – We examined 219 *Schistosoma* samples from 24 countries
98 (Figure 1A). Just over 80% (n=176) of the samples were collected as part of this study with the
99 remaining 43 samples made available through open access resources. Median genome coverage
100 per sample was 29.7x. After filtering, the final dataset contained 35,817,757 total SNVs, 7,206,957
101 common (minor allele frequency; MAF>0.05%) SNVs, and 446,162 common unlinked SNVs
102 genotyped from 162 samples (141 *S. haematobium* and 21 *S. bovis*; Figure 1B). Filtered samples

103 (n=51) were removed due to low genome coverage (mean = 9.7x) compared to passing samples
104 (mean=30.8x). NCBI Short Read Archive (SRA) accessions and sample metadata are available
105 in Supplemental Table 1.

106

107 Population structure and ancestry - We examined relationships among samples with a PCA of
108 355,715 unlinked, common, autosomal SNVs (Figure 1C). Each of our samples fell into one of 3
109 K-means clusters along PC1 and PC2. The three clusters corresponded with (a) *S. haematobium*
110 individuals from northern Africa, (b) southern Africa, and (c) all *S. bovis* samples. The northern
111 population includes samples collected in Cameroon, Cote d' Ivoire, Egypt Gambia, Guinea
112 Bissau, Liberia, Mali, Niger, Nigeria, Senegal and Sudan. The southern population includes
113 samples collected from Angola, Eswatini, Kenya, Madagascar, Namibia, Tanzania, Uganda,
114 Zambia, and Zanzibar. In general, the equator approximately delineates the northern and
115 southern populations. The division of *S. haematobium* into northern and southern populations
116 was consistent among analyses with one exception. Madagascar was an intermediate population
117 in Admixture analysis (k=3) (Supplemental Figure 2). In the PCA, samples from Madagascar area
118 assigned to the southern cluster, but they form a distinct subgroup that is intermediate between
119 the remaining southern and northern samples.

120

121 No samples were placed intermediate between the *S. haematobium* and *S. bovis* clusters which
122 would indicate F1 *S. haematobium-bovis* hybrids among these samples. The weighted, Weir and
123 Cockerham F_{ST} ^{23,24} between the *S. bovis* and *S. haematobium* samples was high ($F_{ST} \geq 0.74$ -
124 0.79). We observed strong subdivision between northern and SE *S. haematobium* populations
125 ($F_{ST} = 0.16$; Figure 1C) with multiple F_{ST} peaks (Figure 2D). There were 275,657 SNVs showing
126 fixed differences ($F_{ST} = 1$) between *S. bovis* and *S. haematobium* (Supplemental Table 2). Mean
127 sequence divergence (d_{XY}) between *S. haematobium* and *S. bovis* was 0.015 compared to 0.002
128 between the northern and southern *S. haematobium* populations (Supplemental Figure 1).

129

130 We used Admixture v1.3.0²⁵ to quantify ancestry among the samples (Figure 1D, Supplemental
131 Figure 2). We found that when $k = 2$, *S. bovis* and south African *S. haematobium* individuals were
132 exclusively assigned with different ancestry components. By contrast *S. haematobium* samples
133 collected from northern Africa were a composite of the two population components including 0.5-
134 26.2% (median = 4.2%) of the *S. bovis* population component (Supplemental Figure 3).

135

136 Reference biases - We tested the data for read-mapping reference biases, which could occur if
137 non-*haematobium* species map poorly to the Egyptian-strain *S. haematobium* reference
138 assembly (GCF_000699445.3), which groups with the northern population in our analyses.
139 Mapping rates were 77.7%, 82.8% and 76.3% for *S. bovis*, northern *S. haematobium* and
140 southern *S. haematobium* populations (Figure 1A). A *t*-Test failed to identify differential mapping
141 rates between *S. haematobium* and *S. bovis* ($p = 0.397$), suggesting that reference bias does not
142 significantly contribute to the results observed. The modest mapping rate results from the
143 complexity of the genome which contains high levels of repetitive elements²⁶.

144

145 Phylogenetics - The species tree generated using SVDquartets and nuclear SNVs revealed a
146 well-resolved topology. We examined 2,500,000 random quartets, representing 8.82% of all
147 possible distinct quartets. Of these, 18.5% ($n = 463,571$) were incompatible with the final tree
148 (Figure 3). *S. haematobium* and *S. bovis* were resolved into two clades and *S. haematobium*
149 individuals fell into clades reflecting geographic relationships.

150

151 On average, we were able to assemble 15,558.4 bp of the mitochondrial genome for each sample,
152 4,757 of which were phylogenetically informative sites. The mitochondrial phylogeny (Figure 4)
153 reveals two major mitochondrial haplotypes, one containing *S. haematobium* individuals from
154 across Africa and another clade containing all of the *S. bovis* and 38 north African *S.*
155 *haematobium*. The presence of *S. haematobium* samples within a larger *S. bovis* clade is
156 consistent with *S. bovis* mitochondrial introgression into *S. haematobium* that has been frequently
157 reported in field samples, for example²⁷. Within the *S. bovis* clade, all *S. haematobium* samples
158 with the introgressed *S. bovis* mitochondria fell into two monophyletic groups, clades “A” and “B”.
159 mtDNA haplotypes from these two clades were from samples widely distributed in northern Africa.
160 For example, the same clade “A” haplotype was found in samples from Egypt, Niger and Cote d’
161 Ivoire (>3,300 km apart). The clade “B” haplotype was found in Niger, Nigeria and Cote d’ Ivoire,
162 a linear distance of 1,171 km. Bootstrap support for each of these major clades was strong
163 (100%). Phylogenetic trees in Newick format are available in the supplementary materials.

164

165 Hybridization and Introgression - We used four methods to identify signatures of hybridization and
166 introgression between *S. haematobium* and *S. bovis*. These methods include f_3 , *D*-statistic, local
167 ancestry assignment (RFmix²⁸) and phylogenetic discordance (TWISST²⁹). First, a negative f_3 (N:
168 S, Sb; $f_3 = -0.128$, SE= $0.8e^{-3}$, z-score=-156.4) indicates that north African *S. haematobium*
169 population include *S. bovis* ancestry. Next, we used the *D*-statistic to test for introgression

170 between *S. haematobium* and *S. bovis* while accounting for lineage sorting (Figure 2E). We
171 averaged D in 10Kb blocks. D was significantly positive ($D=0.46$, $\sigma_M=0.007$, $n=30,278$) indicating
172 biased introgression between north African *S. haematobium* and *S. bovis*.

173
174 We examined the landscape of introgression across the genome using local ancestry with
175 RFmix. We used 38 southern African *S. haematobium* lacking *S. bovis* introgression and 13 *S.*
176 *bovis* samples to serve as reference panels for “pure” *S. haematobium* and *S. bovis*. RFmix
177 results showed that ancestry across the genome was not uniformly distributed in the north African
178 population (Figure 2A). Within the north African population, *S. bovis* ancestry blocks ranged in
179 frequency from 0-100% at any particular locus. Each north African *S. haematobium* sample
180 contained 4.1-22.0% *S. bovis* ancestry (median 7.0%). By comparison the median *S. bovis*
181 ancestry was 0.02% and 100% in the southern *S. haematobium* and *S. bovis* control samples,
182 respectively.

183
184 We used TWISST v67b9a66²⁹ as an independent method for identifying local introgression.
185 TWISST measures shifting gene tree frequencies across the genome. Trees were generated from
186 37,200 non-overlapping, 10kb, sliding windows. On average (mean) each window contained
187 657.3 SNVs. We examined the three possible topologies between northern *S. haematobium*,
188 southern *S. haematobium* and *S. bovis* using *S. margrebowiei* (GCA_944470205.2³⁰) as an
189 outgroup (Figure 2B). The expected species tree, with a monophyletic clade of *S. haematobium*,
190 sister to *S. bovis* was the most common with a mean weight of 0.876 across the genome. The
191 discordant topology uniting northern *S. haematobium* and *S. bovis* was the second most abundant
192 topology (weight = 0.085) compared to the topology with southern *S. haematobium* and *S. bovis*
193 (weight = 0.039).

194
195 We examined the genome for regions that are devoid of introgressed *S. bovis* alleles in the
196 northern *S. haematobium* population. There were 918 genomic deserts lacking *S. bovis* alleles
197 with a median size of 35.8Kb (Figure 2F). With log transformation and robust Z-scores we
198 identified 19 genomic deserts that were significant outliers in terms of length ranging from 1.13-6
199 Mb (median 1.67 Mb). Thirteen of the 19 deserts were on the ZW scaffold and accounted for 32%
200 (28.6 Mb) of its total length.

201
202 Introgression profiles in different countries - We examined the pattern of introgression in individual
203 countries of north Africa (Supplemental Figure 4) as determined by RFMix. The overall patterns

204 of introgression across the genome were consistent between north African populations. Pairwise
205 comparisons of introgressed allele frequencies between countries were positively correlated ($r =$
206 0.59-0.8; Supplemental Figure 5) despite distances spanning up to 3,000 km.

207

208 Impact of introgression on nucleotide diversity and genetic differentiation of *S. haematobium* - We
209 masked introgressed alleles within individual genomes, and recalculated π , F_{ST} and a PCA
210 (Figure 5). Prior to masking, mean nucleotide diversity (π), was 2.3-fold greater in the northern
211 ($\pi = 2.991 \times 10^{-3}$) vs southern ($\pi = 1.278 \times 10^{-3}$) *S. haematobium*, and π was 3.3-fold greater in
212 *S. bovis* ($\pi = 8.329 \times 10^{-3}$) than the entirety of *S. haematobium* ($\pi = 2.523 \times 10^{-3}$). After masking,
213 northern African *S. haematobium* nucleotide diversity was reduced to nearly identical levels seen
214 in the south population: $\pi_{NW} = 2.991 \times 10^{-3}$ to $\pi_{NW} = 1.07 \times 10^{-3}$. By comparison, removing
215 introgressed alleles had minimal impact on F_{ST} ($F_{ST} = 0.154$) between northern and southern *S.*
216 *haematobium*. Additionally, the structure of the PCA was retained, demonstrating that
217 introgression makes a minimal contribution to genome-wide differentiation between northern and
218 southern populations.

219

220 Dating Introgression - We used the size of introgressed haplotype blocks to estimate the number
221 of generations since hybridization for each *S. haematobium* sample in north Africa (Supplemental
222 Figure 6). This gave estimated hybridization dates of ~257-879 generations ago (Median – 426
223 generations, 95% confidence intervals = 281.6-764 generations). *S. haematobium* generation
224 time varies from 3-4³¹ months in lab populations, but is estimated to be 6-12 months in wild
225 populations³². These generation times imply that admixture between *S. haematobium* and *S.*
226 *bovis* occurred ~106 years ago assuming four generations per year (high transmission) or 426
227 years assuming one generation per year (low and / or seasonal transmission). Dating estimates
228 varied between countries: median estimates are lowest in Egypt (286.9) and highest in Nigeria
229 (565) despite their relatively close proximity. A one-way ANOVA indicated significant differences
230 in the number of generations since hybridization between countries (p-value = 1.3e⁻¹⁰;
231 Supplemental Figure 6).

232

233 Selection and adaptive introgression - We examined *S. haematobium* and *S. bovis* populations
234 for signatures of selection using normalized, xpEHH (Figure 2C). We found 996 statistically
235 significant xpEHH values after multiple test correction. We combined values within 1Mb to identify
236 15 genome regions with signatures of positive selection in the northern population and five in the

237 southern population (Supplemental Table 3). The median normalized xpEHH in each of these
238 regions was >6 and the windows ranged in size from 3 bp to 709,928 bp (mean 139,942 bp).

239

240 We combined selection and introgression analyses to identify genome regions showing evidence
241 for adaptive introgression of *S. bovis* alleles into the northern *S. haematobium* population. These
242 regions contained outlier values for selection (xpEHH), elevated Patterson's D ($D \geq 0$) indicative
243 of introgression, high levels of *S. bovis* ancestry ($>95\%$) and significant differentiation from
244 southern *S. haematobium* ($F_{ST} \geq 95^{\text{TH}}$ percentile). Two genome regions met these criteria;
245 chromosome four (NC_067199.1:28,476,500-28,813,500) and chromosome five
246 (NC_067200.1:9,773,000-10,447,000). These genome regions span 1.01 Mb and 15 genes; eight
247 on chr four and seven on chr five (Table 1). Of the 74,955 SNVs in these regions, 989 are
248 nonsense or missense mutations. We found 37 missense SNVs where the *S. bovis* allele is at or
249 near fixation in the northern population (Supplemental Table 4). All of these variants are on chr
250 four and fall within four genes; leishmanolysin-like peptidase, a Rho GTPase-activating protein
251 35, Jumonji domain-containing protein six (JMJD6_4), and Jumonji domain-containing protein six
252 (JMJD6_3).

253

254 **Discussion**

255 Our analysis of >38 million SNVs provides compelling evidence that *S. haematobium* and *S. bovis*
256 are genetically well differentiated. This conclusion is supported by multiple lines of evidence: high
257 F_{ST} values ($F_{ST} \geq 0.74$ -0.79; Figure 1C; Figure 2D), distinction by PCA (Figure 1C), strong
258 differentiation by ancestry components in Admixture analyses (Figure 1D) and well supported
259 monophyletic clades in the nuclear species tree (Figure 3). The agreement between these
260 approaches suggests that strong barriers to gene flow exist between these two species.

261

262 Our analysis revealed that northern African *S. haematobium* are genetically differentiated ($F_{ST} =$
263 0.16) from the southern population. The boundary between these populations appears to extend
264 from Cameroon, Gabon, the Central African Republic, South Sudan, and Ethiopia (Figure 5A) and
265 approximately follows the equator. When introgressed *S. bovis* alleles were removed from
266 genomic data, F_{ST} between these populations is only marginally affected ($F_{ST} = 0.154$). Hence,
267 introgressed *S. bovis* alleles have a minimal impact on genetic differences between the northern
268 and southern populations.

269

270 Our results suggest barriers to gene flow exist between northern and southern *S. haematobium*.
271 The southern *S. haematobium* clade is nested within a larger clade of northern African *S.*
272 *haematobium* (Figure 3). This indicates that *S. haematobium* originated in one of the northern
273 African countries and is consistent with previous work that identified the Arabian Peninsula/Asia
274 as a potential ancestral source population³³. It is possible that the two populations are defined by
275 the distribution of their intermediate hosts. Regional differences in parasite compatibility with their
276 intermediate snail hosts can occur within limited geographical areas³⁴. *S. haematobium* is
277 primarily transmitted by members of the *Bulinus truncatus/tropicus* complex from North Africa and
278 the Middle East are primarily transmitted by the *Bulinus truncatus/tropicus* species complex and
279 parasites from the Afro-tropical region are transmitted by snails of the *Bulinus globosus* and
280 member of the *africanus* species group³⁵, although exceptions to this rule exist³⁶. *S. bovis* by
281 comparison is transmitted by many of the same snail species including members of the *B.*
282 *truncatus/tropicus* and *africanus* species groups, and *B. forskali*²¹. Other, less frequently studied
283 species may influence these dynamics as well^{37,38}. If a barrier exists that is related to the
284 intermediate snail hosts, it has important implications for our understanding of the ecological and
285 epidemiological factors that shape the distribution and dynamics of these two parasite
286 populations. Further investigation at the population boundaries may provide new insights into
287 biological differences and incompatibilities between northern and southern *S. haematobium*
288 populations. We note that the existence of northern and southern populations of *S. haematobium*
289 based on the use of snail intermediate hosts was suggested in the last century³⁹.

290
291 Four aspects of our results support a historical introgression hypothesis. First, each of the north
292 African *S. haematobium* samples contain low levels of *S. bovis* ancestry with the exception of the
293 sole Cameroonian sample. Percentages of *S. bovis* ancestry per individual are similar across
294 multiple analyses: introgressed haplotype blocks from RFMix account for 4.1-22% of individual
295 genomes in the northern *S. haematobium* population, while the population component associated
296 with *S. bovis* in Admixture ranges from 5-26.2% at *K*=2.

297
298 Second, the landscape of introgressed alleles across the genome is consistent across north
299 African samples (Supplemental Figure 4) and positively correlated (Supplemental Figure 5)
300 despite being separated by \leq 3,000 Km. For this profile to be conserved across such a broad
301 distance suggests (A) it occurred in an ancestor of the north African *S. haematobium* or (B)
302 introgressed alleles provided a selective advantage that spread throughout the north African
303 population. Our data support the later with the nuclear phylogeny (Figure 3). The southern

304 population is a monophyletic clade that lacks introgressed *S. bovis* alleles, although the limitations
305 of a bifurcating tree should be considered under scenarios of introgression. We also observe that
306 some introgressed alleles have reached high frequency in the north African population and show
307 signs of selection (Figure 2). Finally, our data suggest that there is a barrier to gene flow/migration
308 between northern and southern *S. haematobium* populations, restricting dispersal of introgressed
309 alleles to the southern population.

310

311 Third, mitochondrial DNA provides insights into a minimal number of hybridization events. 58% of
312 northern *S. haematobium* samples contain introgressed *S. bovis* mitochondria (Figure 4). If the
313 introgressed *S. bovis* mitochondria were the result of contemporary hybridization, we would
314 expect sister relationships between *S. bovis* and *S. haematobium* at the terminal branches of the
315 tree. However, we find that introgressed *S. haematobium* individuals with introgressed *S. bovis*
316 mitochondrial genomes form two monophyletic clades. Clade “A” contains samples from Egypt,
317 Niger, and Cote d’ Ivoire, and Clade “B” contains samples from Niger, Nigeria, and Cote d’ Ivoire;
318 each clade spanning >1,000 Km. The most parsimonious interpretation of the phylogeny is that
319 the introgressed *S. bovis* mitochondria share two distinct origins and imply at least two admixture
320 events resulting from mating between a *S. bovis* female and *S. haematobium* male that occurred
321 in the distant past. We note that laboratory crosses between *S. haematobium* are often
322 asymmetric, and may only produce offspring when male *S. haematobium* are mated with female
323 *S. bovis*⁴⁰ or produce more male offspring³¹. As females are the heterogametic sex, F1 females
324 are expected to show reduced fitness as predicted by Haldane’s rule⁴¹. This may contribute to the
325 limited number of *S. bovis* mtDNA lineages observed in *S. haematobium* populations.

326

327 Fourth, introgressed *S. bovis* nuclear loci are heavily fragmented within the *S. haematobium*
328 genomes indicating multiple generations since introgression. Our estimates of time since
329 introgression span 257-879 generations ago (95% confidence interval). Introgressed loci were
330 measured in tens of kilobases (median = 76.3 Kb) and the largest blocks extended into the
331 megabases (max = 4.05 Mb). This contrasts with early generation hybrids which would have
332 introgressed block lengths spanning, or nearly spanning entire chromosomes⁴² which range in
333 size from 19,481 Kb – 93,306 Kb. One Nigerian sample contained ~25% introgressed DNA,
334 consistent with expectations for a F2 backcross. However, the maximum introgressed fragment
335 size in a Nigerian sample was only 2.83 Mb and median block size in these samples ranged from
336 47.1-97.6 Kb indicating multiple recombination events. We found that the time since introgression
337 was significantly different between multiple countries (Figure 6). For example, neighboring

338 countries Niger (453 generations) and Nigeria (565 generations) were not significantly different,
339 but introgression in Cote d' Ivoire (385 generations) appears to have occurred more recently. The
340 variation in the estimates of generations since introgression are consistent with several regional
341 introgression events. Alternatively, variation in age estimates between countries could reflect
342 extrinsic factors like seasonality or intervention strategies that could lengthen or reduce
343 generation times within sub-populations. If this were the cause, it is possible that the number of
344 generations that have lapsed since an introgression event may vary between countries. Nigerian
345 samples contained, significantly higher levels of introgression than other countries (Kruskal-Wallis
346 H test statistic = 7915, P-value = 0.0049; Supplemental Figure 3): further analyses of Nigerian
347 samples will be of considerable interest.

348

349 Two caveats are needed. First, our age estimates are based on the size of introgressed fragments
350 and assume neutrality. This assumption is violated, because we see some introgressed segments
351 are under positive selection, while others are purged resulting in introgression deserts. Violation
352 of the neutrality assumption may add uncertainty to our age estimates. Second, given that
353 hybridization and introgression has occurred in the past, and that hybridization can be staged in
354 the laboratory⁴³, we might expect that hybridization events may also be ongoing. One
355 interpretation of the fragmented landscape of introgressed *S. bovis* DNA within *S. haematobium*
356 genomes is that this results from an equilibrium between newly introgressed DNA, and selective
357 removal (or selection for) introgressed DNA. Importantly, with both the historical and equilibrium
358 models, the small size of introgressed fragments is clearly consistent with rare introgression, and
359 levels of resulting interspecific gene flow are insufficient to reduce high levels of genetic
360 differentiation between these species.

361

362 *S. bovis* shows 3.3-fold higher diversity than *S. haematobium*, while genetic diversity (π) is 2.3-
363 fold greater in the north *S. haematobium* population than in the south African *S. haematobium*
364 population. When the introgressed *S. bovis* alleles are removed from the analyses, this difference
365 in genetic diversity between the north and south *S. haematobium* populations is reduced to just
366 1.05-fold and π is not significantly different (Figure 5B). By contrast, F_{ST} values between northern
367 and southern *S. haematobium* are consistent whether introgressed alleles are considered (F_{ST} =
368 0.16) or not (F_{ST} = 0.154) and the relationship among samples in the PCAs is nearly identical
369 when introgressed alleles are included or excluded. These results indicate (i) that the elevated π
370 in northern African *S. haematobium* results from *S. bovis* introgression and (ii) that northern and

371 southern *S. haematobium* populations are well differentiated even after removing introgressed *S.*
372 *bovis* alleles.

373
374 Given that introgressed *S. bovis* alleles have persisted in the northern *S. haematobium*
375 population, we examined the data for signals of adaptive introgression. We found two introgressed
376 genome regions with signals of positive selection in the northern population on chr four
377 (NC_067199.1:28,348,440-28,877,530) and chr five (NC_067200.1:9,712,340-10,514,400).
378 Despite the convergence of signals to these regions, we were not able to identify variants driving
379 selection in these regions. We found 37 missense SNVs where the *S. bovis* allele was nearly
380 fixed in the northern population, but none withstood multiple test correction for directional
381 selection. These variants occur in four genes (WormBaseParaSite v18.0⁴⁴), a Rho GTPase-
382 activating protein 35 ($n_{SNVs} = 30$; MS3_00007803) a Leishmanolysin-like peptidase ($n_{SNVs} = 4$;
383 MS3_00007802), and two members of the Jumonji domain-containing protein 6 family; JMJD6_4
384 ($n_{SNVs} = 1$; MS3_00010935) and JMJD6_3 ($n_{SNVs} = 2$; MS3_00010934). The same
385 Leishmanolysin-like peptidase (Table 1) has been identified as a candidate for adaptive
386 introgression from *S. bovis* into *S. haematobium* in two previous studies^{15,16}. Genes in same
387 invadolysin gene family are known to modulate the snail host immune system in *Schistosoma*
388 *mansonii*^{45,46} and this particular gene has been associated with cell migration and invasion in other
389 parasitic taxa⁴⁷.

390
391 We also observed genomic regions on three chromosomes of the *S. haematobium* samples
392 where *S. bovis* introgression is rare or absent (Figure 2F). These introgression deserts may
393 contain hybrid incompatibility loci that result in reduced fitness of early generation hybrids and
394 present barriers to further introgression. Thirteen of the 19 regions occur on the scaffold
395 representing the Z and W sex chromosomes. Eight of the deserts, including the largest occurs
396 within the non-recombining Z-specific region of the sex chromosome. This is consistent with the
397 purging of introgressed blocks containing deleterious alleles in non-recombining regions of the
398 sex chromosomes⁴⁸ which could lead to female sterility as predicted by Haldane's rule.

399
400 Understanding hybridization and introgression between *S. haematobium* and *S. bovis* is important
401 for disease control. If hybridization between these species is infrequent, then there may be
402 minimal benefit in linking strategies that manage both human (*S. haematobium*) and livestock (*S.*
403 *bovis*) *Schistosoma* species. Consistent with this, our results from these samples suggest that
404 hybridization between these species is rare, and gene flow between these species is limited.

405 However, adaptive introgression has introduced *S. bovis* alleles into *S. haematobium* populations.
406 This is a clear example of alleles being transferred between livestock and human parasites
407 through introgression. Some *S. bovis* alleles have reached high frequency and are likely
408 selectively advantageous. Future work should aim to understand how the introgressed *S. bovis*
409 variants contribute to the fitness of *S. haematobium* individuals. The strong differentiation
410 between northern *S. haematobium* populations, carrying introgressed *S. bovis* alleles and
411 southern *S. haematobium* populations, with no introgression, is of particular interest. Additionally,
412 future work should examine differences between northern and southern *S. haematobium*
413 populations, and test whether they are reproductively isolated.

414

415 Several limitations to our study and its conclusions should be noted. First, recombination rates
416 have not been quantified in *S. haematobium* so our estimates of age of admixture are based on
417 recombination rates measured in *Schistosoma mansoni*⁴⁹. To improve the accuracy of these
418 estimates, direct measures of recombination rates from *S. haematobium* genetic crosses are
419 needed. Second, our results pertain to *S. haematobium* and *S. bovis*. Extant hybridization
420 between other schistosome species (*S. haematobium*/*S. guineensis* and *S. bovis*/*S. curassoni*)
421 have been documented in field collected samples with genomic data^{50,51}. Our results suggest that
422 *Schistosoma* species pairs may form a spectrum in hybridization frequency and compatibility.
423 Future work to understand the factors that impact hybridization and present barriers to gene flow
424 between schistosomes species pairs will be of great interest, and can provide a more nuanced
425 understanding of hybridization and potential implications for schistosome control.

426

427 **Online Methods**

428

429 Sample collection: description, ethics, and identification – We used samples or data from three
430 sources. i) The first dataset was generated from samples provided by the Schistosomiasis
431 Collection At the Natural History Museum⁵² which is housed at the Natural History Museum
432 (London). SCAN samples consisted of individual miracidia and cercariae preserved on Whatman
433 FTA cards⁵³. We analyzed 114 *S. haematobium* and *S. bovis* samples from 123 individual hosts
434 (snails or humans) and 12 Africa countries. ii) In addition to the SCAN samples, we collected nine
435 adult *Schistosome* worms, presumed to be *S. bovis*, from the intestines of routinely slaughtered
436 cattle from meat vendors at three abattoirs located in Auchi, Benin City, and Enugu in Nigeria. In
437 the laboratory, the mesenteric vessels of each purchased intestines were visually inspected for
438 schistosome parasites. Adult schistosomes were recovered using forceps and washed in saline

439 solution. Adult pairs were separated into males and females before being stored in 96% ethanol
440 for subsequent DNA isolation analyses. iii) Finally, for the third source of data we used whole
441 genome sequence data from NCBI^{15,16,18,22,26,30}.

442

443 Samples provided by the SCAN repository were originally collected in accordance with protocols
444 approved by local, state, and national authorities, including the Ministry of Health. The Imperial
445 College Research Ethics Committee (ICREC) at Imperial College London, in conjunction with
446 ongoing Schistosomiasis Control Initiative (SCI) activities, provided additional ethical guidance
447 for samples collected through the CONTRAST program. Ethical clearance and study protocols
448 for Nigerian samples were approved by the National Health Research Ethics Committee of Nigeria
449 (NHREC) (protocol number: NHREC/01/01/2007– 30/10/2020 and approval number:
450 NHREC/01/01/2007– 29/03/2021) and the Institutional Review Board (IRB) of University of Texas
451 Health, San Antonio Texas, United States of America (protocol number: HSC20180612H).
452 Informed consent was obtained from all participants, with processes tailored to ensure
453 understanding and voluntary participation. All data were anonymized to protect participant
454 privacy, and schistosomiasis-positive individuals were treated with a single dose of praziquantel
455 (40 mg/kg). For livestock parasite collection, approval was secured from local veterinarians. No
456 animals were euthanized for research purposes; *Schistosoma* samples were collected during
457 routine activities at abattoirs. Further details on collection methods, ethical approvals, and data
458 availability for public samples can be found in their respective publications documented in
459 Supplemental Table 1.

460

461 Provisional species identifications were assigned to cercariae and miracidia based on sampled
462 host. For example, miracidia hatched from eggs collected from human urine samples were
463 assumed to be *S. haematobium* while miracidia hatched from eggs in cattle feces were assumed
464 to be *S. bovis*. Cercariae collected from snails were identified by Sanger sequencing the
465 mitochondrial cox1 region and the ribosomal internal transcribed spacer (ITS) rDNA region as
466 previously described²¹. Downstream genetic analysis with whole genome SNVs was used to
467 confirm and reassign species identifications where necessary.

468

469 Library prep and sequencing – DNA from single parasites stored on FTA cards was subjected to
470 whole-genome amplification (WGA) using methods previously described in⁵³. DNA was extracted
471 from single male adult *S. bovis* worms using the DNeasy® Blood and Tissue kit before
472 subsequent WGA. We quantified amount of schistosome DNA in each WGA sample by real time

473 quantitative PCR (qPCR) reactions using the single copy gene α -tubulin 1 gene markers primers
474 (*S. haematobium*: forward [GGT GGT ACT GGT TCT GGT TT], reverse [AAA GCA CAA TCC
475 GAA TGT TCT AA]; *S. bovis*: forward [ATG GCC TCG TTA TCA ACC AT], reverse [TGG CCT
476 CGT TAT CAA CCA TA] following previously described protocol in ⁵³. DNA sequencing libraries
477 were generated from 500 ng of DNA per sample using the KAPA Hyperplus kit protocol with the
478 following modifications: i) enzymatic fragmentation at 37°C for 10 minutes, ii) adapter ligation at
479 20°C for an hour, and iii) 4 cycles of library PCR amplification. After qPCR quantification of each
480 library with KAPA Library Quantification Kits, samples with similar concentrations were combined
481 into pools for sequencing at 4nM, while samples with disparate concentrations were equalized in
482 10 mM Tris-HCl pH 8.5 before pooling. Libraries were sequenced with 150 bp paired-end reads
483 on two Illumina NovaSeq flowcell. All resulting reads were deposited in the NCBI Short Read
484 Archive under BioProject PRJNA636746 and are documented in Supplemental Table 1.

485

486 Computing environment - Analyses were conducted on the Texas Biomedical Research Institute's
487 high-performance computing cluster, with worker nodes containing 96 cores and 1 TB of memory.
488 Computational environments were managed using Conda v22.9.0. Environmental recipe files,
489 Jupyter notebooks, and other code can is archived on GitHub
490 ([github.com/nealplatt/sch_hae_scan v0.1z](https://github.com/nealplatt/sch_hae_scan)) and at <https://doi.org/10.5281/zenodo.13124719>.

491

492 Read filtering and Mapping - Raw reads were quality trimmed with trimmomatic v0.39 ⁵⁴ using the
493 following parameters: LEADING:10, TRAILING:10, SLIDINGWINDOW:4:15, MINLEN:36,
494 ILLUMINACLIP:2:30:10:1:true. This command removed low quality bases at the beginning and
495 ends of the reads, removed portions of the read where quality dropped below a minimum
496 threshold, trimmed adapter sequences and discarded reads <36 nts. We then mapped the
497 trimmed reads to the Egyptian-strain *S. haematobium* reference genome, GCF_000699445.3²²,
498 with BBMap v38.18⁵⁵. On average the *S. haematobium* and *S. bovis* (GCA_944470425.1)
499 genome assemblies are ~97% similar across their genomes¹⁸ which should minimally affect
500 reference biases when mapping short reads. However, to avoid reference biases we used the
501 'vslow' and 'minid=0.8' options with BBMap and discarded ambiguously mapping reads
502 ('ambig=toss').

503

504 Genotyping, phasing, and filtering - Mapped reads were sorted with SAMtools v1.13⁵⁶ and
505 checked for duplicates with GATK v4.2.0.0's⁵⁷ mark_duplicates. Then single nucleotide variants
506 (SNVs) were genotyped with HaplotypeCaller and GenotypeGVCFs. To make the dataset more

507 manageable, we genotyped each chromosome separately using the -L option. Next, we removed
508 all indels and hard filtered SNVs based on QualByDepth ("QD < 2.0"), RMSMappingQuality (MQ
509 < 30.0), FisherStrand (FS > 60.0), StrandOddsRation (SOR > 3.0), MappingQualityRankSumTest
510 (MQRankSum < -12.5), and ReadPosRankSumTest (ReadPosRankSum < -8.0) with GATK's
511 VariantFiltration. We removed multi-allelic sites, and sites with genotype quality (GQ) <20 or read
512 depth (DP) <8 with VCFtools v0.1.16⁵⁸. After these filters were applied we removed genomic
513 sites that were genotyped in ≤50% of individuals and then any individuals that were genotyped at
514 ≤50% of sites.

515

516 SNVs on each chromosome were phased using Beagle v 5.2_21Apr21.304⁵⁹ in windows of 20
517 cM and a 10 cM overlap. Currently there are no direct measures of recombination rate in *S.*
518 *haematobium*. The best available data is from *S. mansoni*⁴⁹ which has and a map length of 1134.8
519 cM and an estimated recombination rate (physical-to-map distance) of 244.2 Kb/cM. The genome
520 assemblies for *S. mansoni* (GCA_000237925.5) and *S. haematobium* (GCF_000699445.3) are
521 similar in length, 391 Mb vs 400 Mb respectively so assuming a uniform recombination rate similar
522 to *S. mansoni* across the genome, these values are comparable to a 4.88 Mb window and a 2.4
523 Mb step size⁴⁹. We used a burn in of 20 iterations and 60 iterations for the phasing run. All phased
524 chromosome VCFs were combined into a single file using vcfcombine from vcflib v1.0.3⁶⁰ before
525 an additional round of post-phase filtering.

526

527 In some cases, multiple miracidia were analyzed from a single host potentially adding highly
528 related samples to our dataset and skewing the downstream results. To remove these, we
529 examined kinship coefficients in our samples using the autosomal chromosomes and the “-
530 unrelated” function in king v2.2.7⁶¹. This parameter identifies second-degree relatives within the
531 dataset that can be removed prior to downstream analyses. Next, we generated a set of SNVs
532 that were common (minor allele frequency; MAF > 0.05) and unlinked. Unlinked loci were filtered
533 with Plink v1.90b6.21⁶² by removing linked SNVs with a pairwise $r^2 > 0.2$. This filter was applied
534 in 25 Kb sliding windows with a 5kb steps. Finally, we used SnpEff v5.1⁶³, to identify the impact
535 of these SNVs on the amino acid sequence in coding regions. To do this we imported the *S.*
536 *haematobium* reference genome (GCF_000699445.3) along with the associated GenBank
537 annotations to create a custom database.

538

539 Principal Component Analyses - We used a series of tools to explore population structure in our
540 data sets. We used common (minor allele frequency; MAF>0.05), unlinked, autosomal SNVs and

541 Plink v1.90b6.21⁶² to generate a principal component analysis (PCA) to examine relationships
542 among the samples. We used a *K*-means clustering algorithm to assign each sample to between
543 1 and 10 populations with the Kmeans() function in sklearn.cluster v1.2.0⁶⁴. We then used the
544 Elbow method⁶⁵ to examine distortion in the model and determine the optimal number of clusters
545 in the data. Once we identified the optimal number of clusters, we assigned each sample within
546 a cluster, and those designations were used to differentiate the *S. haematobium* populations using
547 analyses as below. These cluster assignments were also used validate the assumed species
548 identify of each sample.

549

550 Admixture - We examined the ancestry of each sample with Admixture v1.3.0²⁵ and the same
551 unlinked, autosomal SNV dataset from the PCA analyses. However, we further thinned the SNV
552 data with VCFtools v0.1.16⁵⁸ ensuring that no two SNVs were within 10kb of each other. This step
553 minimizes any potential effects of linkage on the results. We ran Admixture v1.3.0²⁵, allowing for
554 2 to 20 possible population components, and used the cross-validation error to determine the
555 optimal range⁶⁶. Additionally, we randomly selected individuals with $\geq 99.999\%$ *S. bovis* or *S.*
556 *haematobium* ancestry in the *k*=2 analysis to serve as reference samples for each species in
557 downstream analyses.

558

559 Nucleotide diversity (π), Sequence divergence (d_{XY}), and Fixation index (F_{ST}) - We used scikit-
560 allel v1.3.5⁶⁷ to calculate nucleotide diversity (π), sequence divergence (d_{XY}), and the fixation
561 index (F_{ST}) in sliding windows of 10 kb using autosomal SNVs allel.windowed_diversity(),
562 allele.windowed_divergence, and allel.windowed_weir_cockerham_fst() functions. The weighted,
563 Weir-Cockerham F_{ST} ^{23,24} was measured between species (*S. haematobium* vs. *S. bovis*) and
564 between the *K*-means populations. Next, we used the reference panel, described above, to
565 identify ancestry informative sites between the *S. haematobium* and *S. bovis* samples. We used
566 scikit-allel v1.3.5's⁶⁷ allel.weir_cockerham_fst() to calculate F_{ST} at individual sites. Only sites
567 where $F_{ST} = 1$ were retained.

568

569 Biogeography – *S. haematobium* was split into two groups based on the *K*-means clustering
570 analysis of the PCA results. At *k*=2 Admixture differentiated *S. haematobium* and *S. bovis*
571 samples, but at *k*=3 Admixture broadly confirmed the presence of two different *S. haematobium*
572 populations. We used the admixture proportion (Q) from *k*=3, to visualize how the populations
573 were distributed across Africa. The presence of this ancestry component was extrapolated into
574 unsampled geographic regions using the OrdinaryKriging() function implemented in pykrige

575 v1.7.0 with a linear variogram model⁶⁸. Geographic distances between samples were calculated
576 with the haversine() v2.8.0 function (<https://pypi.org/project/haversine/>).

577

578 Genome-wide tests for introgression - We used a series of tests to explore the presence of
579 introgression between *S. bovis* and the *S. haematobium* populations. First, we used
580 average_patterson_f3() from scikit-allel v1.3.5⁶⁷ to calculate a normalized f_3 ⁶⁹ averaged across
581 blocks of 500 SNVs. Next, we tested for gene flow using the D -statistic, also known as the ABBA
582 BABA test⁷⁰. We used *S. margrebowiei* (GCA_944470205.2³⁰) as the outgroup (O), *S. bovis* as
583 the donor population (P3), and the *S. haematobium* K -means populations as the recipients (P1
584 and P2). We measured D across the genome in 500 SNV blocks with moving_patterson_d() in
585 scikit-allel v1.3.5⁶⁷. Introgressed loci were defined when $D > 0 + 2\sigma$.

586

587 Local Ancestry Assignment - For local ancestry assignment, we used RFMix v2.03-r0²⁸ and
588 TWISST v67b9a66²⁹. RFMix v2.03-r0²⁸ uses a random forest approach to assign local ancestry
589 to genomic segments by comparing samples to reference panels. For this, we used the reference
590 samples selected from the Admixture analyses. We generated a genetic map using a uniform
591 recombination rate estimated from *S. mansoni* crosses (1 centimorgan = 287,000 bp⁴⁹). The
592 remainder of the parameters were set to the default.

593

594 TWISST v67b9a66²⁹ uses gene trees sampled from across the genome to identify potentially
595 introgressed loci. It does this by iteratively sampling subtrees from the gene tree and calculating
596 relative support for each of the possible species trees. We generated gene trees from loci
597 containing 500, phased, common (MAF >0.05) SNVs with RAxML-NG v1.1⁷¹. For each locus we
598 searched for the 10 best trees and then bootstrapped the best tree for 100 replicates using the
599 GTR+ASC_LEWIS substitution model and *S. margrebowiei* as an outgroup. Nodes supported in
600 ≤10 bootstrap replicates were collapsed with Newick Utilities v1.6⁷². The collapsed trees were
601 used as input for TWISST v67b9a66²⁹. Samples were assigned to their K -means population.

602

603 Selection - We compared selection in the *S. haematobium* intra populations using cross-
604 population extended haplotype homozygosity (xpEHH⁷³). Unphased xpEHH was measured with
605 selscan v2.0.0⁷⁴. The resulting unphased xpEHH values were normalized with norm v1.3.0 and
606 the '--xpehh flag'. Bonferroni corrected p-values were assigned to each site. Sites with a corrected
607 p-value < 0.01 were considered to be experiencing putative directional selection between the two
608 *S. haematobium* populations.

609

610 Identifying putative adaptive introgression –We searched the genome for regions with F_{ST} ,
611 Patterson's D, local ancestry, and xpEHH values indicative of adaptive introgression. To do this
612 we examined how these values were distributed across the genome in sliding windows of 337 Kb
613 and 3,370 bp step size; values equivalent to 1% and 0.01% of the autosomal genome.
614 Specifically, we were looking for regions of the genome that are among the most highly
615 differentiated between the two schistosome populations ($F_{ST} \geq 95^{\text{th}}$ percentile), with statistically
616 significant signals of introgression (Patterson's D > 0) and directional selection (xpEHH p-value $<$
617 0.01), and the *S. bovis* alleles are at high frequency in the northern or southern *S. haematobium*
618 populations ($>95\%$). Patterson's D was measured under the assumed 4-taxon tree (((southern
619 *S. haematobium*, northern *S. haematobium*), *S. bovis*), *S. margrebowiei*). Windows that met these
620 criteria were then merged together if they were within 10Kb of each other to identify loci containing
621 signals of adaptive introgression.

622

623 Autosomal Species Tree - To better understand the relationships among the samples, used
624 SVDquartets⁷⁵ as implemented in PAUP* v4.0.a.build166⁷⁶ to generate a species tree.
625 SVDQuartets has been shown to perform well in the presence of gene flow as was suspected
626 here⁷⁷. We examined 2.5m random quartets along with 100 standard bootstrap replicates. Nodes
627 in the gene trees supported by $<10\%$ of bootstrap replicates were collapsed Newick Utilities
628 v1.6⁷².

629

630 Dating introgression - Recombination acts to continuously break down introgressed haplotypes.
631 As a result, the size of introgressed haplotype blocks is directly related to the number or
632 generations since hybridization⁷⁸. This can be roughly estimated with the formula $G=1/LP$ where
633 G is generations, L is the average length of introgression haplotypes in Morgans, and P is the
634 proportion of the genome from the major parent⁷⁹. We identified introgressed blocks and their
635 lengths (L) for each individual with RFMix v2.03-r0²⁸ and P was estimated using Admixture
636 (represented as q). A one-way ANOVA was used to identify differences in age estimates between
637 populations (countries).

638

639 Introgression Deserts – Some regions of the genome may be resistant to introgression. This could
640 present as large regions lacking introgressed alleles. We used the RFMix results to identify
641 regions of the genome where *S. bovis* ancestry was 0% in the north African *S. haematobium*

642 populations. We log-transformed the length of each region and assigned robust Z-scores. Putative
643 introgression deserts were regions with robust Z-scores > 3.

644

645 Mitochondrial genome assembly and phylogeny - We used GetOrganelle v1.7.7.0⁸⁰ to *de novo*
646 assemble mitochondrial genomes. Specifically, we used the animal_mt model and 10 rounds of
647 assembly with *k*-mer sizes of 21, 45, 65, 85, and 105. The mitochondrial contigs were then
648 scaffolded with RagTag v2.1.0^{81,82} and RAxML-NG v1.1⁷¹ was used to generate a maximum
649 likelihood tree of the mitochondrial genomes. We used a GTR+G substitution model to and 100
650 starting trees. Nodal support was assessed with 1,000 bootstrap replicates.

651

652 **Acknowledgements**

653 We thank Sandy Smith and John Heaner for providing computational support at Texas Biomedical
654 Research Institute's High-Performance Computing Cluster. We would like to thank Frederic
655 Chevalier, Winka Le Clec'h, and Kathrin Bailey for providing feedback during the course of this
656 project. This research was funded by the National Institute of Allergy and Infectious Diseases
657 (NIAD R01 AI166049-01). Schistosomiasis Collections at the Natural History Museum (SCAN)
658 was supported by Wellcome Trust grant 1045958/Z/13/Z. The field work referenced in this study
659 relied on various organizations and funding bodies across multiple countries. In Angola, funding
660 was provided by the Calouste Gulbenkian Foundation in collaboration with the Centro de
661 Investigação em Saúde de Angol, the Programa Nacional de Doenças Tropicais Negligenciadas
662 and the Ministério da Saúde de Angola. In Côte d'Ivoire and Niger, the research was funded by
663 SCORE through the Bill & Melinda Gates Foundation, RISEAL-Niger, Université Félix Houphouët-
664 Boigny, and the Centre Suisse de Recherches Scientifiques en Côte d'Ivoire. The Eswatini
665 National Control Program, Environmental Health Unit, and the School Health Program contributed
666 significantly to the work in Eswatini. The CONTRAST project in Kenya, Uganda, and Zambia was
667 funded by the European Commission, the Kenya Medical Research Institute, National Museums
668 of Kenya, Uganda Ministry of Health, and the University of Zambia. In Liberia, the UK Department
669 for International Development provided funding via SCI (now Unlimit Health) and the Ministry of
670 Health of Liberia. Madagascar's efforts were funded through SCAN, Unlimit Health, and the
671 Madagascar Ministry of Public Health. Work in Namibia was funded by the END Fund and the
672 Namibia Ministry of Health and Social Services. In Zanzibar, the ZEST project was funded by
673 SCORE, the Ministry of Health (Zanzibar), and the Public Health Laboratory—Ivo de Carneri,
674 Pemba.

675

676 Individual collectors are listed in the Supplemental Table 1.

677

678 **Author Contributions**

679 Roy N Platt II: Conceptualization, Formal Analysis, Writing – Original Draft, Writing - Review &
680 Editing. Elisha Enabulele: Conceptualization, Formal Analysis, Investigation, Resources, Writing
– Original Draft, Writing - Review & Editing. Ehizogie Adeyemi: Resources. Marian O Agbugui:
682 Resources. Oluwaremilekun G Ajakaye: Resources. Ebube C Amaechi: Resources. Chika E
683 Ejikeugwu: Resources. Christopher Igbeneghu: Resources. Victor S Njom: Resources. Precious
684 Dlamini: Resources. Grace A. Arya: Investigation. Robbie Diaz: Investigation. Muriel Rabone:
685 Resources, Writing - Review & Editing. Fiona Allan: Resources, Writing - Review & Editing.
686 Bonnie Webster: Resources, Writing - Review & Editing. Aidan Emery: Resources, Writing -
687 Review & Editing. David Rollinson: Resources, Writing - Review & Editing. Timothy J.C.
688 Anderson: Conceptualization, Formal Analysis, Writing – Original Draft, Writing - Review &
689 Editing, Supervision.

690

691 **Competing interests**

692 The authors declare no competing interests.

693

694 **Corresponding authors**

695 Correspondence to Roy N. Platt II or Timothy J. C. Anderson.

696 **References**

- 697 1 Taylor, S. A. & Larson, E. L. Insights from genomes into the evolutionary importance and
698 prevalence of hybridization in nature. *Nature ecology & evolution* **3**, 170-177,
699 doi:10.1038/s41559-018-0777-y (2019).
- 700 2 Aguillon, S. M., Dodge, T. O., Preising, G. A. & Schumer, M. Introgression. *Current biology : CB*
701 **32**, R865-r868, doi:10.1016/j.cub.2022.07.004 (2022).
- 702 3 Edelman, N. B. & Mallet, J. Prevalence and Adaptive Impact of Introgression. *Annual review of*
703 *genetics* **55**, 265-283, doi:10.1146/annurev-genet-021821-020805 (2021).
- 704 4 Mixão, V. & Gabaldón, T. Hybridization and emergence of virulence in opportunistic human
705 yeast pathogens. *Yeast (Chichester, England)* **35**, 5-20, doi:10.1002/yea.3242 (2018).
- 706 5 Depotter, J. R., Seidl, M. F., Wood, T. A. & Thomma, B. P. Interspecific hybridization impacts host
707 range and pathogenicity of filamentous microbes. *Current opinion in microbiology* **32**, 7-13,
708 doi:10.1016/j.mib.2016.04.005 (2016).
- 709 6 Ravazi, A. *et al.* Climate and Environmental Changes and Their Potential Effects on the Dynamics
710 of Chagas Disease: Hybridization in Rhodniini (Hemiptera, Triatominae). *Insects* **14**,
711 doi:10.3390/insects14040378 (2023).

712 7 King, K. C., Stelkens, R. B., Webster, J. P., Smith, D. F. & Brockhurst, M. A. Hybridization in
713 Parasites: Consequences for Adaptive Evolution, Pathogenesis, and Public Health in a Changing
714 World. *PLoS pathogens* **11**, e1005098, doi:10.1371/journal.ppat.1005098 (2015).

715 8 Colley, D. G., Bustinduy, A. L., Secor, W. E. & King, C. H. Human schistosomiasis. *Lancet (London, England)* **383**, 2253-2264, doi:10.1016/s0140-6736(13)61949-2 (2014).

716 9 Webster, B. L., Diaw, O. T., Seye, M. M., Webster, J. P. & Rollinson, D. Introgressive hybridization
717 of Schistosoma haematobium group species in Senegal: species barrier break down between
718 ruminant and human schistosomes. *PLoS Negl Trop Dis* **7**, e2110,
719 doi:10.1371/journal.pntd.0002110 (2013).

720 10 Webster, J. P. *et al.* Parasite Population Genetic Contributions to the Schistosomiasis
721 Consortium for Operational Research and Evaluation within Sub-Saharan Africa. *The American
722 journal of tropical medicine and hygiene* **103**, 80-91, doi:10.4269/ajtmh.19-0827 (2020).

723 11 Léger, E. *et al.* Prevalence and distribution of schistosomiasis in human, livestock, and snail
724 populations in northern Senegal: a One Health epidemiological study of a multi-host system. *The
725 Lancet. Planetary health* **4**, e330-e342, doi:10.1016/s2542-5196(20)30129-7 (2020).

726 12 Huyse, T. *et al.* Bidirectional introgressive hybridization between a cattle and human
727 schistosome species. *PLoS pathogens* **5**, e1000571, doi:10.1371/journal.ppat.1000571 (2009).

728 13 Sene-Wade, M., Marchand, B., Rollinson, D. & Webster, B. L. Urogenital schistosomiasis and
729 hybridization between Schistosoma haematobium and Schistosoma bovis in adults living in
730 Richard-Toll, Senegal. *Parasitology* **145**, 1723-1726, doi:10.1017/s0031182018001415 (2018).

731 14 Díaz, A. V., Walker, M. & Webster, J. P. Reaching the World Health Organization elimination
732 targets for schistosomiasis: the importance of a One Health perspective. *Philosophical
733 transactions of the Royal Society of London. Series B, Biological sciences* **378**, 20220274,
734 doi:10.1098/rstb.2022.0274 (2023).

735 15 Platt, R. N. *et al.* Ancient Hybridization and Adaptive Introgression of an Invadolysin Gene in
736 Schistosome Parasites. *Molecular biology and evolution* **36**, 2127-2142,
737 doi:10.1093/molbev/msz154 (2019).

738 16 Rey, O. *et al.* Diverging patterns of introgression from Schistosoma bovis across S. haematobium
739 African lineages. *PLoS pathogens* **17**, e1009313, doi:10.1371/journal.ppat.1009313 (2021).

740 17 Djuikwo-Teukeng, F. F. *et al.* Population genetic structure of Schistosoma bovis in Cameroon.
741 *Parasites & vectors* **12**, 56, doi:10.1186/s13071-019-3307-0 (2019).

742 18 Oey, H. *et al.* Whole-genome sequence of the bovine blood fluke Schistosoma bovis supports
743 interspecific hybridization with S. haematobium. *PLoS pathogens* **15**, e1007513,
744 doi:10.1371/journal.ppat.1007513 (2019).

745 19 Boon, N. A. M. *et al.* No barrier breakdown between human and cattle schistosome species in
746 the Senegal River Basin in the face of hybridisation. *International journal for parasitology* **49**,
747 1039-1048, doi:10.1016/j.ijpara.2019.08.004 (2019).

748 20 Kincaid-Smith, J. *et al.* Morphological and genomic characterisation of the Schistosoma hybrid
749 infecting humans in Europe reveals admixture between Schistosoma haematobium and
750 Schistosoma bovis. *PLoS Negl Trop Dis* **15**, e0010062, doi:10.1371/journal.pntd.0010062 (2021).

751 21 Pennance, T. *et al.* Interactions between Schistosoma haematobium group species and their
752 Bulinus spp. intermediate hosts along the Niger River Valley. *Parasites & vectors* **13**, 268,
753 doi:10.1186/s13071-020-04136-9 (2020).

754 22 Stroehlein, A. J. *et al.* Chromosome-level genome of Schistosoma haematobium underpins
755 genome-wide explorations of molecular variation. *PLoS pathogens* **18**, e1010288,
756 doi:10.1371/journal.ppat.1010288 (2022).

757

758 23 Weir, B. S. & Cockerham, C. C. Estimating F-statistics for the analysis of population structure.
759 *Evolution; international journal of organic evolution* **38**, 1358-1370, doi:10.1111/j.1558-
760 5646.1984.tb05657.x (1984).

761 24 Bhatia, G., Patterson, N., Sankararaman, S. & Price, A. L. Estimating and interpreting FST: the
762 impact of rare variants. *Genome Res* **23**, 1514-1521, doi:10.1101/gr.154831.113 (2013).

763 25 Alexander, D. H., Novembre, J. & Lange, K. Fast model-based estimation of ancestry in unrelated
764 individuals. *Genome Res* **19**, 1655-1664, doi:10.1101/gr.094052.109 (2009).

765 26 Young, N. D. *et al.* Whole-genome sequence of *Schistosoma haematobium*. *Nature genetics* **44**,
766 221-225, doi:10.1038/ng.1065 (2012).

767 27 Angora, E. K. *et al.* High prevalence of *Schistosoma haematobium* × *Schistosoma bovis* hybrids in
768 schoolchildren in Côte d'Ivoire. *Parasitology* **147**, 287-294, doi:10.1017/s0031182019001549
769 (2020).

770 28 Maples, B. K., Gravel, S., Kenny, E. E. & Bustamante, C. D. RFMix: a discriminative modeling
771 approach for rapid and robust local-ancestry inference. *American journal of human genetics* **93**,
772 278-288, doi:10.1016/j.ajhg.2013.06.020 (2013).

773 29 Martin, S. H. & Van Belleghem, S. M. Exploring Evolutionary Relationships Across the Genome
774 Using Topology Weighting. *Genetics* **206**, 429-438, doi:10.1534/genetics.116.194720 (2017).

775 30 Comparative genomics of the major parasitic worms. *Nature genetics* **51**, 163-174,
776 doi:10.1038/s41588-018-0262-1 (2019).

777 31 Polack, B. *et al.* Experimental Infections Reveal Acquired Zoonotic Capacity of Human
778 Schistosomiasis Through Hybridization. *The Journal of infectious diseases* **229**, 1904-1908,
779 doi:10.1093/infdis/jiae152 (2024).

780 32 King, C. H., Muchiri, E. M. & Ouma, J. H. Evidence against rapid emergence of praziquantel
781 resistance in *Schistosoma haematobium*, Kenya. *Emerging infectious diseases* **6**, 585-594,
782 doi:10.3201/eid0606.000606 (2000).

783 33 Webster, B. L. *et al.* Genetic diversity within *Schistosoma haematobium*: DNA barcoding reveals
784 two distinct groups. *PLoS Negl Trop Dis* **6**, e1882, doi:10.1371/journal.pntd.0001882 (2012).

785 34 Rollinson, D., Stothard, J. R. & Southgate, V. R. Interactions between intermediate snail hosts of
786 the genus *Bulinus* and schistosomes of the *Schistosoma haematobium* group. *Parasitology* **123**
787 Suppl, S245-260, doi:10.1017/s0031182001008046 (2001).

788 35 Brown, D. S. *Freshwater snails of Africa and their medical importance*. (CRC press, 1994).

789 36 Ratard, R. C. *et al.* Human schistosomiasis in Cameroon. I. Distribution of schistosomiasis. *The
790 American journal of tropical medicine and hygiene* **42**, 561-572, doi:10.4269/ajtmh.1990.42.561
791 (1990).

792 37 Southgate, V. R., Wright, C. A., Laaziri, H. M. & Knowles, R. J. Is *Planorbarius metidjensis*
793 compatible with *Schistosoma haematobium* and *S. bovis*? *Bulletin de la Societe de pathologie
794 exotique et de ses filiales* **77**, 409-506 (1984).

795 38 Mandahl-Barth, G. J. B. o. t. W. H. O. Intermediate hosts of Schistosoma: African Biomphalaria
796 and *Bulinus*: 2. **17**, 1 (1957).

797 39 Webbe, G. & James, C. Infra-specific variations of *Schistosoma haematobium*. *Journal of
798 helminthology* **45**, 403-413, doi:10.1017/s0022149x00000651 (1971).

799 40 Taylor, M. G. Hybridisation experiments on five species of African schistosomes. *Journal of
800 helminthology* **44**, 253-314, doi:10.1017/s0022149x00021969 (1970).

801 41 Haldane, J. B. J. o. g. Sex ratio and unisexual sterility in hybrid animals. **12**, 101-109 (1922).

802 42 Harris, K. & Nielsen, R. The Genetic Cost of Neanderthal Introgression. *Genetics* **203**, 881-891,
803 doi:10.1534/genetics.116.186890 (2016).

804 43 Mathieu-Bégné, E. *et al.* Schistosoma haematobium and Schistosoma bovis first generation
805 hybrids undergo gene expressions changes consistent with species compatibility and heterosis.
806 *PLoS Negl Trop Dis* **18**, e0012267, doi:10.1371/journal.pntd.0012267 (2024).
807 44 Harris, T. W. *et al.* WormBase: a modern Model Organism Information Resource. *Nucleic Acids*
808 *Res* **48**, D762-d767, doi:10.1093/nar/gkz920 (2020).
809 45 Hambrook, J. R., Kaboré, A. L., Pila, E. A. & Hanington, P. C. A metalloprotease produced by larval
810 Schistosoma mansoni facilitates infection establishment and maintenance in the snail host by
811 interfering with immune cell function. *PLoS pathogens* **14**, e1007393,
812 doi:10.1371/journal.ppat.1007393 (2018).
813 46 Hambrook, J. R. & Hanington, P. C. A cercarial invadolysin interferes with the host immune
814 response and facilitates infection establishment of Schistosoma mansoni. *PLoS pathogens* **19**,
815 e1010884, doi:10.1371/journal.ppat.1010884 (2023).
816 47 McHugh, B. *et al.* Invadolysin: a novel, conserved metalloprotease links mitotic structural
817 rearrangements with cell migration. *The Journal of cell biology* **167**, 673-686,
818 doi:10.1083/jcb.200405155 (2004).
819 48 Fraïsse, C. & Sachdeva, H. The rates of introgression and barriers to genetic exchange between
820 hybridizing species: sex chromosomes vs autosomes. *Genetics* **217**,
821 doi:10.1093/genetics/iyaa025 (2021).
822 49 Criscione, C. D., Valentim, C. L., Hirai, H., LoVerde, P. T. & Anderson, T. J. Genomic linkage map
823 of the human blood fluke Schistosoma mansoni. *Genome Biol* **10**, R71, doi:10.1186/gb-2009-10-
824 6-r71 (2009).
825 50 Berger, D. J. *et al.* Genomic evidence of contemporary hybridization between Schistosoma
826 species. *PLoS pathogens* **18**, e1010706, doi:10.1371/journal.ppat.1010706 (2022).
827 51 Landeryou, T. *et al.* Genome-wide insights into adaptive hybridisation across the Schistosoma
828 haematobium group in West and Central Africa. *PLoS Negl Trop Dis* **16**, e0010088,
829 doi:10.1371/journal.pntd.0010088 (2022).
830 52 Emery, A. M., Allan, F. E., Rabone, M. E. & Rollinson, D. Schistosomiasis collection at NHM
831 (SCAN). *Parasites & vectors* **5**, 185, doi:10.1186/1756-3305-5-185 (2012).
832 53 Le Clec'h, W. *et al.* Whole genome amplification and exome sequencing of archived schistosome
833 miracidia. *Parasitology* **145**, 1739-1747, doi:10.1017/s0031182018000811 (2018).
834 54 Bolger, A. M., Lohse, M. & Usadel, B. Trimmomatic: a flexible trimmer for Illumina sequence
835 data. *Bioinformatics* **30**, 2114-2120, doi:10.1093/bioinformatics/btu170 (2014).
836 55 Bushnell, B. BBMap: a fast, accurate, splice-aware aligner. (Lawrence Berkeley National
837 Lab.(LBNL), Berkeley, CA (United States), 2014).
838 56 Li, H. *et al.* The Sequence Alignment/Map format and SAMtools. *Bioinformatics* **25**, 2078-2079,
839 doi:10.1093/bioinformatics/btp352 (2009).
840 57 McKenna, A. *et al.* The Genome Analysis Toolkit: a MapReduce framework for analyzing next-
841 generation DNA sequencing data. *Genome Res* **20**, 1297-1303, doi:10.1101/gr.107524.110
842 (2010).
843 58 Danecek, P. *et al.* The variant call format and VCFtools. *Bioinformatics* **27**, 2156-2158,
844 doi:10.1093/bioinformatics/btr330 (2011).
845 59 Browning, B. L., Tian, X., Zhou, Y. & Browning, S. R. Fast two-stage phasing of large-scale
846 sequence data. *American journal of human genetics* **108**, 1880-1890,
847 doi:10.1016/j.ajhg.2021.08.005 (2021).
848 60 Garrison, E., Kronenberg, Z. N., Dawson, E. T., Pedersen, B. S. & Prins, P. A spectrum of free
849 software tools for processing the VCF variant call format: vcflib, bio-vcf, cyvcf2, hts-nim and
850 slivar. *PLoS Comput Biol* **18**, e1009123, doi:10.1371/journal.pcbi.1009123 (2022).

851 61 Manichaikul, A. *et al.* Robust relationship inference in genome-wide association studies. **26**,
852 2867-2873 (2010).

853 62 Purcell, S. *et al.* PLINK: a tool set for whole-genome association and population-based linkage
854 analyses. *American journal of human genetics* **81**, 559-575, doi:10.1086/519795 (2007).

855 63 Cingolani, P. *et al.* A program for annotating and predicting the effects of single nucleotide
856 polymorphisms, SnpEff: SNPs in the genome of *Drosophila melanogaster* strain w1118; iso-2;
857 iso-3. *Fly* **6**, 80-92, doi:10.4161/fly.19695 (2012).

858 64 Pedregosa, F. *et al.* Scikit-learn: Machine learning in Python. **12**, 2825-2830 (2011).

859 65 Kodinariya, T. M. & Makwana, P. R. J. I. J. Review on determining number of Cluster in K-Means
860 Clustering. **1**, 90-95 (2013).

861 66 Evanno, G., Regnaut, S. & Goudet, J. J. M. e. Detecting the number of clusters of individuals
862 using the software STRUCTURE: a simulation study. **14**, 2611-2620 (2005).

863 67 scikit-allel: v1.3.5 (2022).

864 68 PyKrig: Development of a Kriging Toolkit for Python (2014).

865 69 Patterson, N. *et al.* Ancient admixture in human history. *Genetics* **192**, 1065-1093,
866 doi:10.1534/genetics.112.145037 (2012).

867 70 Green, R. E. *et al.* A draft sequence of the Neandertal genome. *Science (New York, N.Y.)* **328**,
868 710-722, doi:10.1126/science.1188021 (2010).

869 71 Kozlov, A. M., Darriba, D., Flouri, T., Morel, B. & Stamatakis, A. RAxML-NG: a fast, scalable and
870 user-friendly tool for maximum likelihood phylogenetic inference. *Bioinformatics* **35**, 4453-4455,
871 doi:10.1093/bioinformatics/btz305 (2019).

872 72 Junier, T. & Zdobnov, E. M. The Newick utilities: high-throughput phylogenetic tree processing in
873 the UNIX shell. *Bioinformatics* **26**, 1669-1670, doi:10.1093/bioinformatics/btq243 (2010).

874 73 Sabeti, P. C. *et al.* Genome-wide detection and characterization of positive selection in human
875 populations. *Nature* **449**, 913-918, doi:10.1038/nature06250 (2007).

876 74 Szpiech, Z. (bioRxiv, 2021).

877 75 Chifman, J. & Kubatko, L. Identifiability of the unrooted species tree topology under the
878 coalescent model with time-reversible substitution processes, site-specific rate variation, and
879 invariable sites. *Journal of theoretical biology* **374**, 35-47, doi:10.1016/j.jtbi.2015.03.006 (2015).

880 76 Swofford, D. L. J. h. p. c. f. e. PAUP: phylogenetic analysis using parsimony (and other methods),
881 version 4.0 beta. (2002).

882 77 Long, C. & Kubatko, L. The Effect of Gene Flow on Coalescent-based Species-Tree Inference.
883 *Systematic biology* **67**, 770-785, doi:10.1093/sysbio/syy020 (2018).

884 78 Harrison, R. G. & Larson, E. L. Hybridization, introgression, and the nature of species boundaries.
885 *The Journal of heredity* **105 Suppl 1**, 795-809, doi:10.1093/jhered/esu033 (2014).

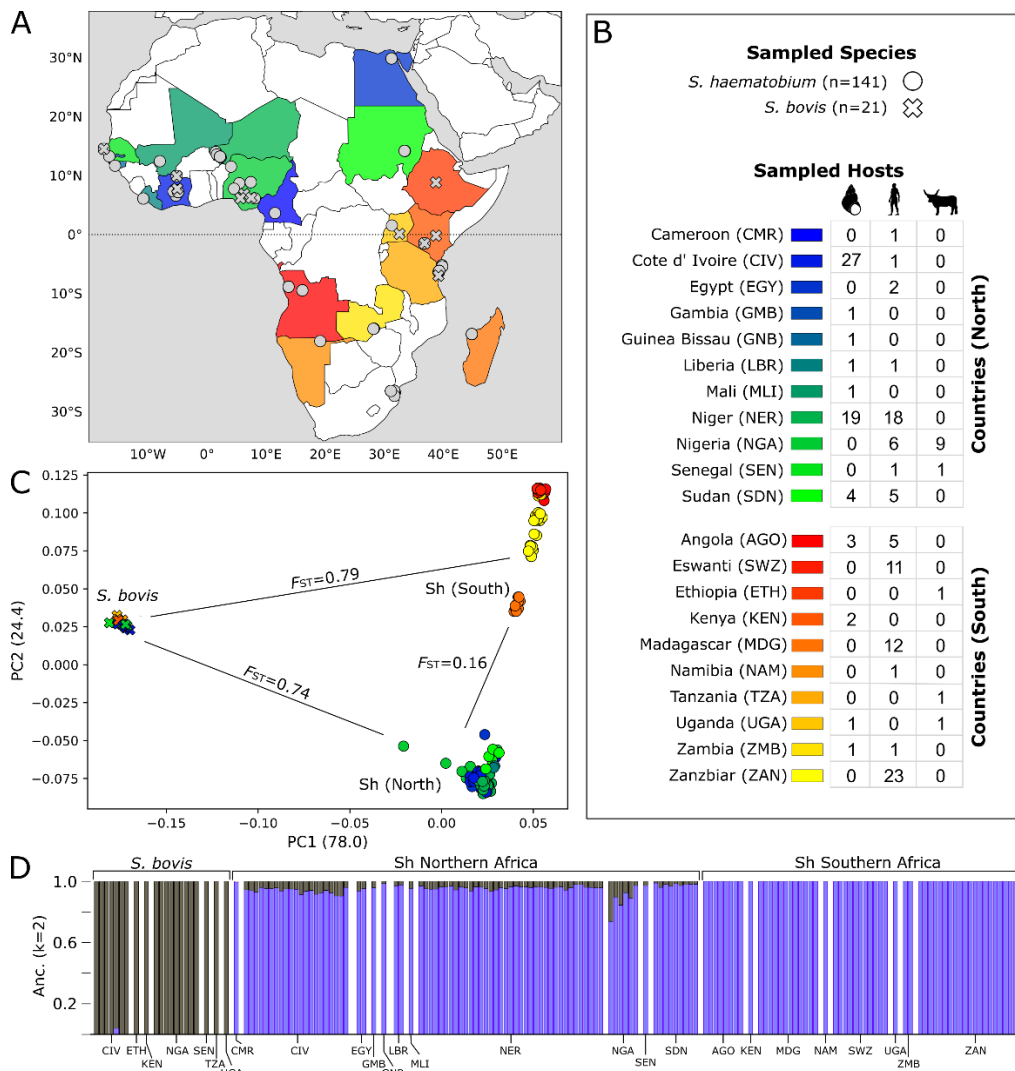
886 79 Schumer, M., Cui, R., Powell, D. L., Rosenthal, G. G. & Andolfatto, P. Ancient hybridization and
887 genomic stabilization in a swordtail fish. *Molecular ecology* **25**, 2661-2679,
888 doi:10.1111/mec.13602 (2016).

889 80 Jin, J. J. *et al.* GetOrganelle: a fast and versatile toolkit for accurate de novo assembly of
890 organelle genomes. *Genome Biol* **21**, 241, doi:10.1186/s13059-020-02154-5 (2020).

891 81 Alonge, M. *et al.* Automated assembly scaffolding using RagTag elevates a new tomato system
892 for high-throughput genome editing. *Genome Biol* **23**, 258, doi:10.1186/s13059-022-02823-7
893 (2022).

894 82 Alonge, M. *et al.* RaGOO: fast and accurate reference-guided scaffolding of draft genomes.
895 *Genome Biol* **20**, 224-224, doi:10.1186/s13059-019-1829-6 (2019).

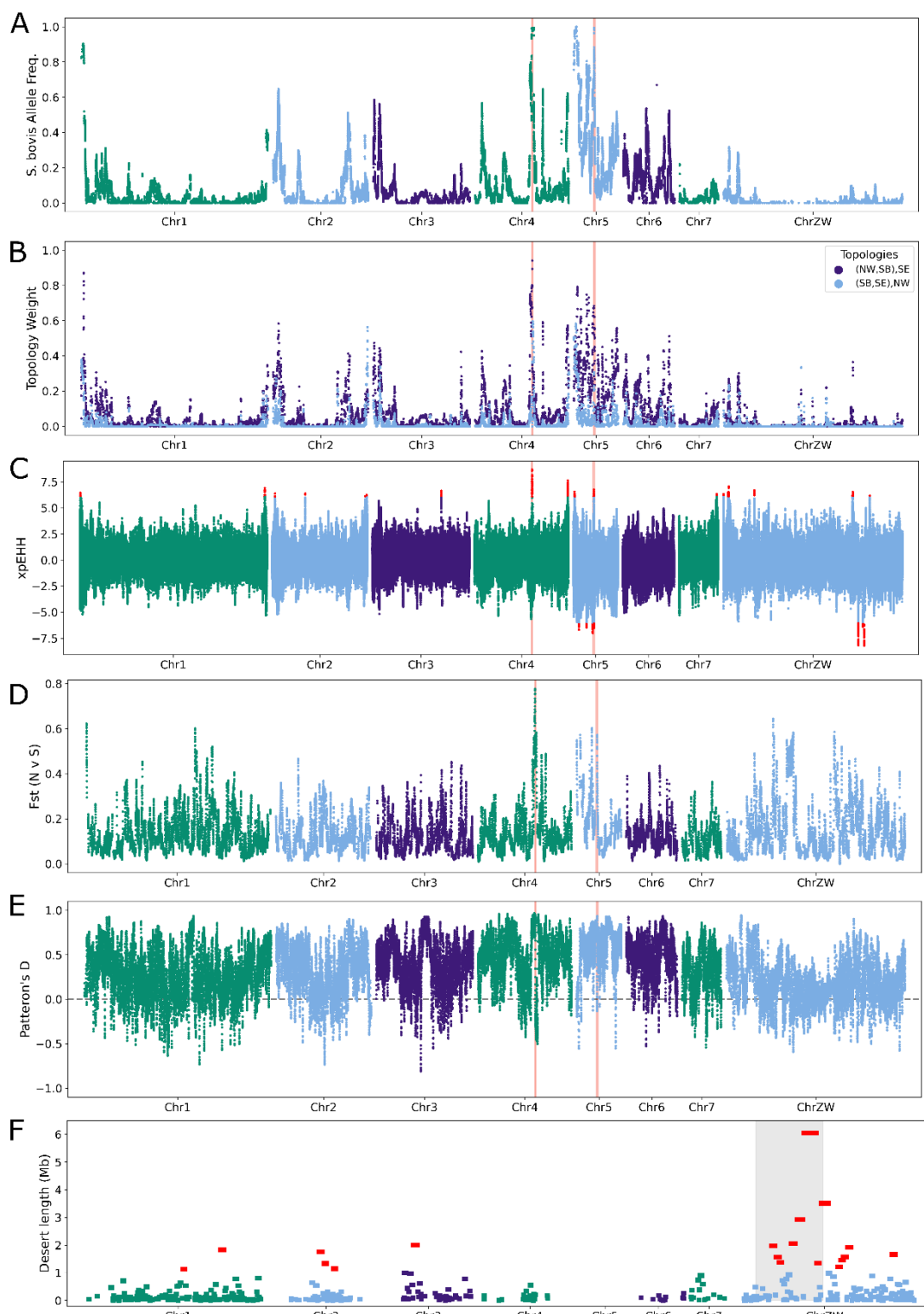
896



897
898

899 **Figure 1. – Sampling localities, sample summary and the population structure of *Schistosoma***
900 ***haematobium* and *S. bovis*.** (A) Collection locations for samples used in this study. Where exact
901 coordinates for samples were not readily available we used the country capital as the collection locality.
902 Two populations of *S. haematobium* were identified; northern and southern. The southern population in
903 red-yellow and the northern population in blue to green. (B) A description of species, hosts, and countries
904 sampled in this study. (C) A principal component analysis of 355,715 unlinked, common (MAF>0.05),
905 autosomal variants. The three clusters correspond to *S. bovis*, and the northern and southern *S.*
906 *haematobium* populations. Weighted, Weir-Cockerham F_{ST} values between these populations are shown.
907 (D) A supervised admixture analysis ($k=2$) was used to assign ancestry to each sample. This analysis
908 shows almost all of the northern *S. haematobium* samples contained low levels of *S. bovis*. Country Codes
909 are as follows: "AGO": Angola, "CMR": Cameroon, "CIV": Cote d'Ivoire, "EGY": Egypt, "SWZ": Eswanti,
910 "ETH": Ethiopia, "GMB": Gambia, "GNB": Guinea Bissau, "KEN": Kenya, "LBR": Liberia, "MDG":
911 "NAM": Namibia, "NER": Niger, "NGA": Nigeria, "SEN": Senegal, "SDN": Sudan,
912 "TZA": Tanzania, "UGA": Uganda, "ZMB": Zambia, "ZAN": Zanzibar.

913



914

915

916

917

918

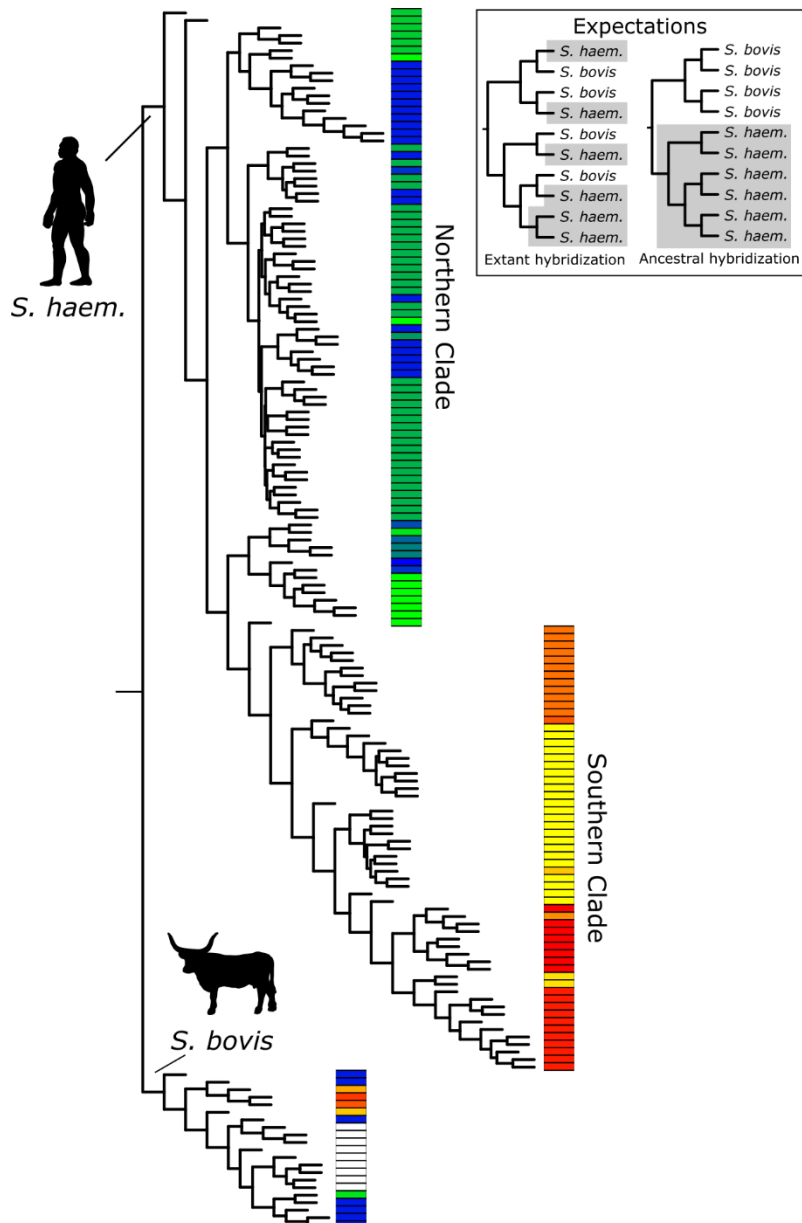
919

920

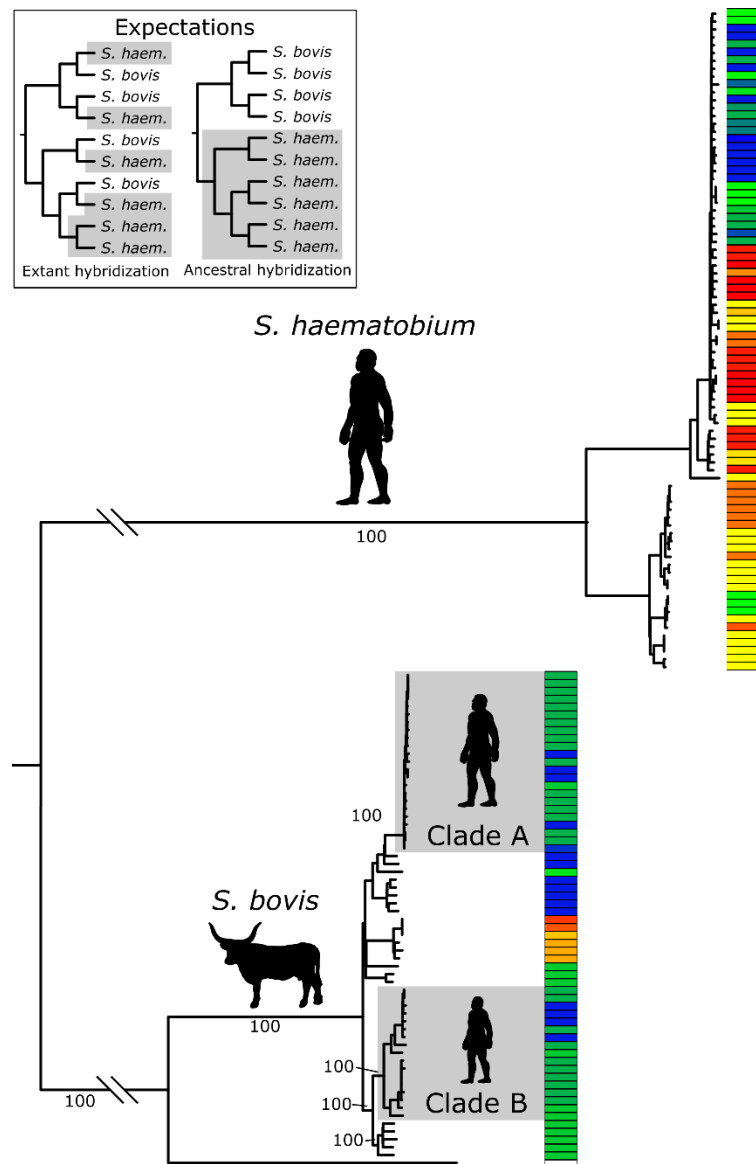
Figure 2. – Local measurements of differentiation, introgression and selection across the genome.

(A) The frequency of *S. bovis* ancestry across the genome in the northern *S. haematobium* population was estimated using RFmix. While the percentage of *S. bovis* alleles in the population is low overall, the *S. bovis* alleles are at or near fixation at loci on Chr4 and Chr5. (B) Gene tree topology weightings across the genome depicting the possible relationships between the northern and south *S. haematobium* populations and *S. bovis* using TWISST. Each locus across the genome is shown as stacked bar plots. While both tools

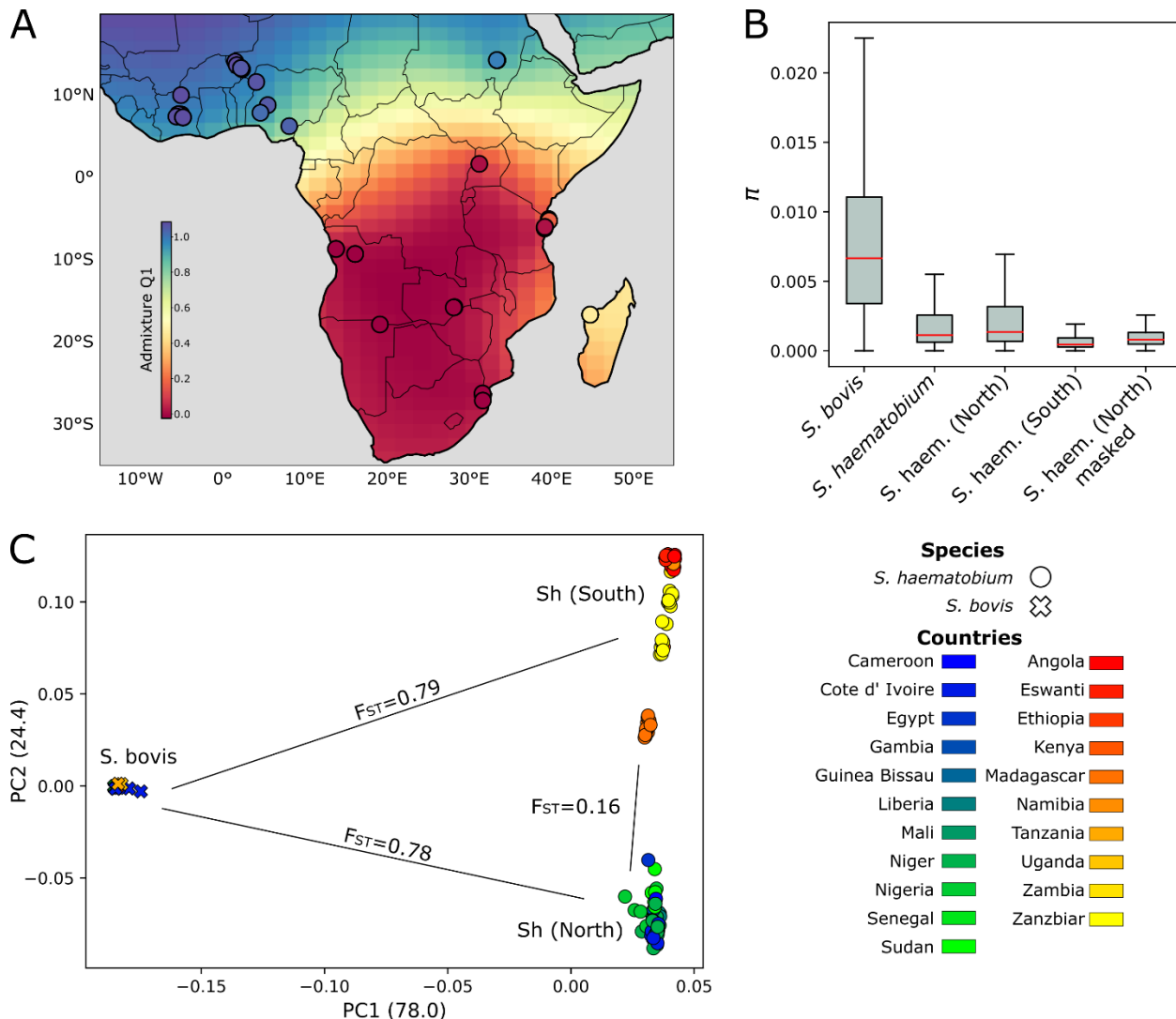
921 use different methods to depict the relationships between these taxa they recover similar results. (C)
922 Differential selection between *S. haematobium* populations was measured across the genome with
923 extended haplotype homozygosity (xpEHH). Positive values indicate positive selection in the northern
924 population and negative values indicate positive selection in the southern population. Significant xpEHH
925 values ($p<0.05$) after multiple test correction are highlighted in red. (D) The weighted Weir-Cockerham
926 fixation index (F_{ST}) between northern and southern Africa, *S. haematobium* populations was measured
927 across the genome in 10Kb windows. These results indicated multiple, highly differentiated regions
928 between the two populations. (E) Patterson's D statistic was measured to determine if high F_{ST} regions
929 were the result of introgressed *S. bovis* alleles present in northern populations using a test tree of
930 (((southern *S. haematobium*, northern *S. haematobium*), *S. bovis*), *S. margrebowiei*). D measured across
931 the genome was significantly positive indicating the presence of gene flow between *S. bovis* and north
932 African *S. haematobium* populations. (F) Multiple regions of the northern African *S. haematobium* genome
933 lacked introgressed *S. bovis* alleles. Introgression desserts that are longer than expected by chance are
934 shown ($Z\text{-score}_{\text{Length}} > 3$) in red. The grey box represents the Z-specific region of the sex chromosome.
935 Results for F_{ST} and Patterson's D are shown after Gaussian smoothing ($\sigma=3$). Pink vertical lines
936 indicate putative regions of adaptive introgression.



938 **Figure 3 – Species tree of *S. haematobium* and *S. bovis* populations –** SVDquartets species tree
939 generated from autosomal SNVs. All nodes were supported by >95% of bootstrap replicates. Phylogenetic
940 relationships between the species can be used to differentiate extant vs ancestral hybridization (inset). The
941 tree shows that both *S. haematobium* and *S. bovis* are monophyletic. Biogeographic partitioning within the
942 tree indicates that *S. haematobium* originated in northern Africa and expanded into southern Africa.
943



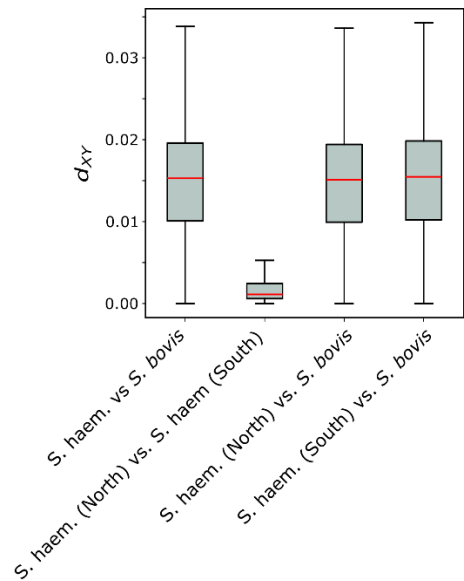
944
945 **Figure 4. Mitochondrial tree of *S. haematobium* and *S. bovis*** - A gene tree was recovered from
946 mitochondrial genome assemblies from each sample. Bootstrap support at select nodes is shown.
947 Phylogenetic relationships between the species can be used to differentiate extant vs ancestral
948 hybridization (inset). Two well supported clades of *S. haematobium* contain an introgressed *S. bovis*
949 mitotype, designated as "A" and "B". Both the "A" and "B" clades contain samples from north Africa. All
950 south African samples are found within a single clade of the remaining *S. haematobium* samples



951

952 **Figure 5 Biogeography of *S. haematobium* is not determined by introgressed *S. bovis* alleles.** *S. haematobium* samples were split into two populations by PCA, Admixture and phylogenetic analyses. (A) 953 We used Kriging interpolation to examine the distribution of these populations across Africa using the 954 population component that differentiates the *S. haematobium* populations from one another (B) Nucleotide 955 diversity (π) was calculated in 10kb sliding windows after masking introgressed *S. bovis* alleles present in 956 the northern *S. haematobium* population. π is higher in the northern African *S. haematobium* compared to 957 the southern population. When introgressed *S. bovis* alleles are masked, π is similar for both the southern 958 and northern populations. (C) After masking introgressed *S. bovis* alleles the PCA is similar to Figure 1C. 959 The similarity between the two PCAs show that the genetic differentiation between the northern and 960 southern *S. haematobium* populations is not driven by introgressed *S. bovis* alleles. 961

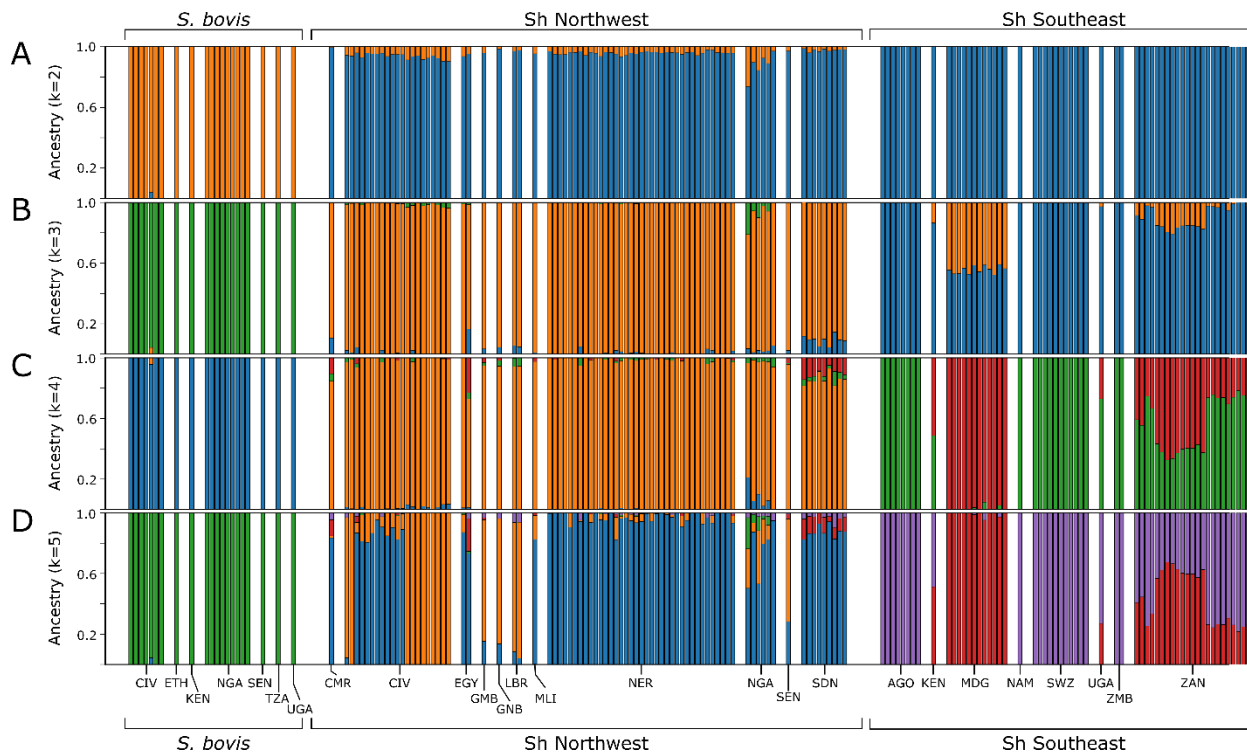
962



963

964 **Supplemental Figure 1.** Sequence divergence (d_{XY}) between *S. bovis* and *S. haematobium*. We
965 examined d_{XY} across the genome in 10Kb windows. Sequence divergence was the same across all
966 comparisons between *S. haematobium* samples and *S. bovis* regardless of the population tested (d_{XY}
967 means = 0.0144-0.0148). By comparison sequence divergence between northern and southern *S.*
968 *haematobium* populations was nearly 7x lower (mean d_{XY} =0.002).

969

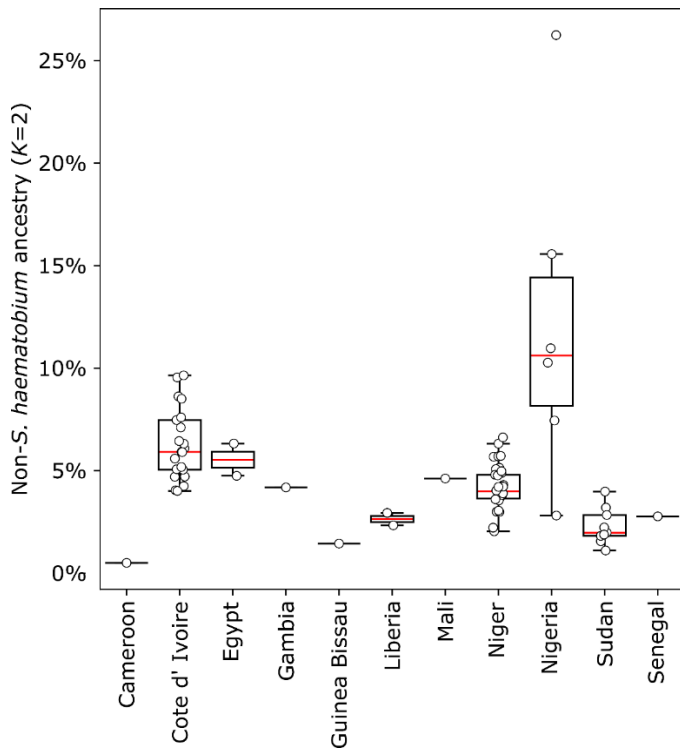


970

971 **Supplemental Figure 2. Whole genome ancestry assignment with Admixture.** We examined multiple
972 different population (k) sizes with Admixture. (A) At k=2, *S. haematobium* and *S. bovis* were separated, and
973 two general populations were identified within the *S. haematobium* samples corresponding to a northern
974 and southern population. We also partitioned the data into (B) three populations (k=3) and (C) four
975 populations. (D) Five populations (k=5) was the optimum number according (Evanno *et al.* 2005). Here the
976 samples show clear distinctions between the two *S. haematobium* populations. Country Codes are as
977 follows: "AGO": Angola, "CMR": Cameroon, "CIV": Cote d' Ivoire, "EGY": Egypt, "SWZ": Eswanti,
978 "ETH": Ethiopia, "GMB": Gambia, "GNB": Guinea Bissau, "KEN": Kenya, "LBR": Liberia, "MDG": Madagascar,
979 "MLI": Mali, "NAM": Namibia, "NER": Niger, "NGA": Nigeria, "SEN": Senegal, "SDN": Sudan, "TZA":
980 Tanzania, "UGA": Uganda, "ZMB": Zambia, "ZAN": Zanzibar.

981

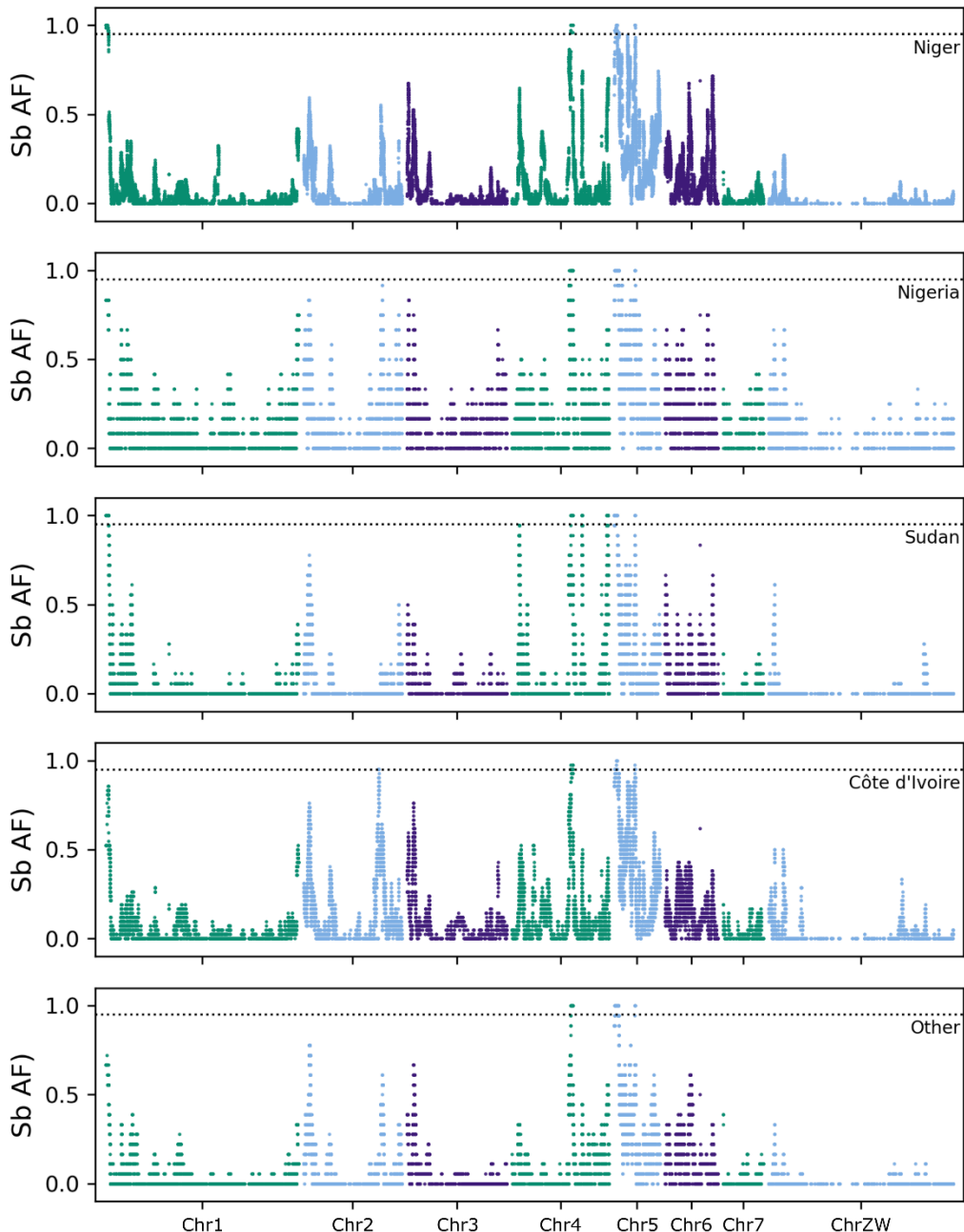
982



983

984 **Supplemental Figure 3. Comparison of non-S. haematobium ancestry calculated from Admixture**
985 **(k=2) in each north African sample** – Ancestry of each sample was assigned to up to two different
986 population components with Admixture. These two components were maximized in samples from southern
987 Africa or S. bovis samples. By comparison, north African samples were a composite of these two
988 populations with low, but varying levels of the S. bovis component found in each individual. The
989 population component corresponding to S. bovis ancestry was significantly higher in Nigerian than in other
990 north African countries (Kruskal-Wallis H test statistic = 7.915, P-value = 0.0049).

991

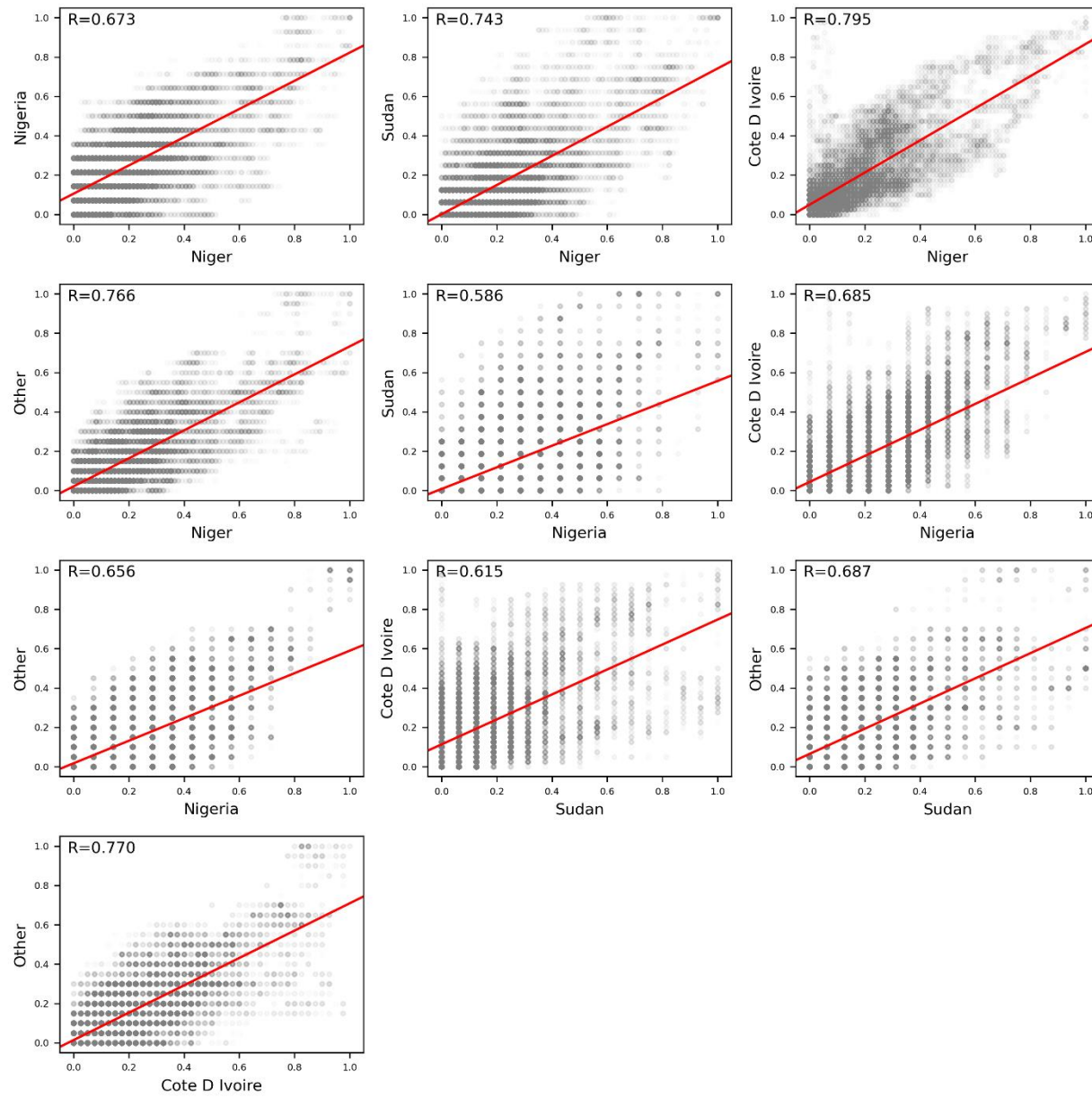


992

993 **Supplemental Figure 4. *S. bovis* allele frequency across the genome within *S. haematobium***
994 **samples from Northern African countries** - The frequency of *S. bovis* ancestry across the genome is
995 shown for each of the northwest African countries. In general, the distribution of *S. bovis* alleles is similar
996 for each population. This consistency is an indicator of historic introgression event(s). The dotted line
997 indicates 95% allele frequency.

998

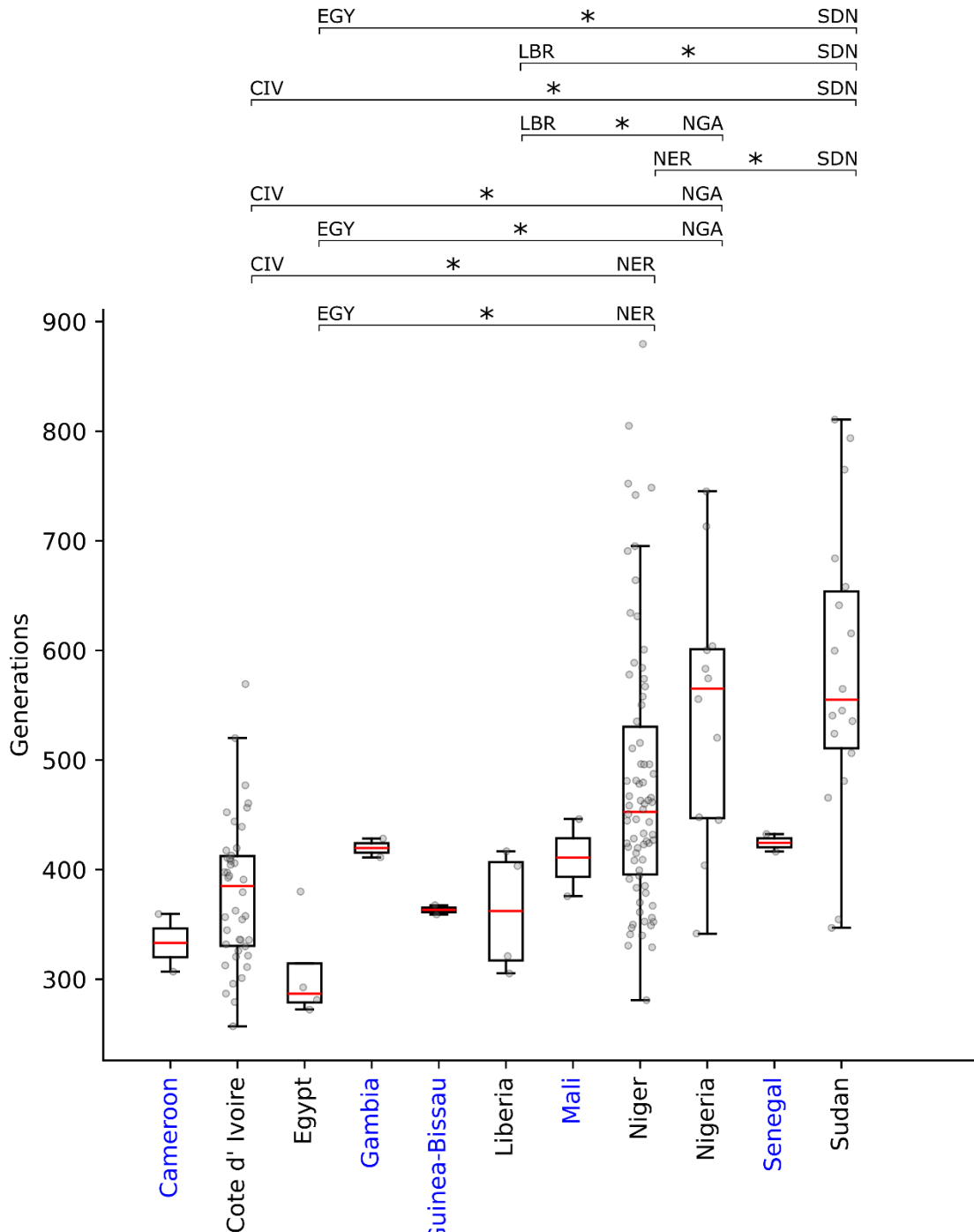
999



1000

1001 **Supplemental Figure 5. Pairwise comparison of introgressed *S. bovis* allele frequencies within**
1002 **northern *S. haematobium* samples by country** – Introgressed *S. bovis* allele frequency is positively
1003 correlated between countries. Pearson's correlation coefficient (R) is >0.586 in all comparisons. The
1004 correlation of introgressed allele frequencies between populations up to 3,338 Km apart is consistent with
1005 older introgression events. .

1006



1007

Supplemental Figure 6 – Estimated number of generations since admixture with *S. bovis*. We estimated the number of generations since admixture for each sample in the northern *S. haematobium* population by examining the length of introgressed *S. bovis* loci within the genomes. Individual estimates for each sample for each country are shown as two grey points, one for each haplotype. Results from a one-way ANOVA indicated that age estimates varied significantly between countries. Countries with a single individual (two haplotypes) are shown in blue and were not included in the ANOVA analyses. A “**” indicates p -values < 0.05 . Differences in ages may indicate multiple introgression events.

1015

Table1. Genes containing outlier loci.

Chrom	Location	Gene_ID	Gene Name
Chr4	NC_067199.1:28466881-28497752	MS3_00007802	Leishmanolysin-like peptidase
Chr4	NC_067199.1:28497929-28529268	MS3_00007803	MS3_00007803
Chr4	NC_067199.1:28531133-28546611	MS3_00007804	RAD50
Chr4	NC_067199.1:28562068-28562732	MS3_00000457	JMJD6_1
Chr4	NC_067199.1:28571061-28634110	MS3_00010935	JMJD6_4
Chr4	NC_067199.1:28662329-28782419	MS3_00010934	JMJD6_3
Chr4	NC_067199.1:28742276-28747614	MS3_00007805	TY3BI_12
Chr4	NC_067199.1:28785057-28816546	MS3_00010936	JMJD6_5
Chr5	NC_067200.1:9933321-9974793	MS3_00011123	MS3_00011123
Chr5	NC_067200.1:9989479-10043873	MS3_00011124	AK2_3
Chr5	NC_067200.1:10117557-10118821	MS3_00011125	MS3_00011125
Chr5	NC_067200.1:10187316-10209172	MS3_00011126	TSC2
Chr5	NC_067200.1:10219534-10229257	MS3_00009120	MDP1_1
Chr5	NC_067200.1:10245731-10246840	MS3_00000691	MS3_00000691
Chr5	NC_067200.1:10414911-10585361	MS3_00011127	MS3_00011127